



HAL
open science

Medium-induced jet evolution: wave turbulence and energy loss

Leonard Fister, Edmond Iancu

► **To cite this version:**

Leonard Fister, Edmond Iancu. Medium-induced jet evolution: wave turbulence and energy loss. Journal of High Energy Physics, 2015, 10.1007/JHEP03(2015)082 . cea-01296867

HAL Id: cea-01296867

<https://cea.hal.science/cea-01296867>

Submitted on 1 Apr 2016

HAL is a multi-disciplinary open access archive for the deposit and dissemination of scientific research documents, whether they are published or not. The documents may come from teaching and research institutions in France or abroad, or from public or private research centers.

L'archive ouverte pluridisciplinaire **HAL**, est destinée au dépôt et à la diffusion de documents scientifiques de niveau recherche, publiés ou non, émanant des établissements d'enseignement et de recherche français ou étrangers, des laboratoires publics ou privés.

Medium–induced jet evolution: wave turbulence and energy loss

Leonard Fister and Edmond Iancu

Institut de Physique Théorique de Saclay, F-91191 Gif-sur-Yvette, France

E-mail: leonard.fister@cea.fr, edmond.iancu@cea.fr

ABSTRACT: We study the gluon cascade generated via successive medium-induced branchings by an energetic parton propagating through a dense QCD medium. We focus on the high-energy regime where the energy E of the leading particle is much larger than the characteristic medium scale $\omega_c = \hat{q}L^2/2$, with \hat{q} the jet quenching parameter and L the distance travelled through the medium. In this regime the leading particle loses only a small fraction $\sim \alpha_s(\omega_c/E)$ of its energy and can be treated as a steady source of radiation for gluons with energies $\omega \leq \omega_c$. For this effective problem with a source, we obtain exact analytic solutions for the gluon spectrum and the energy flux. These solutions exhibit wave turbulence: the basic physical process is a continuing fragmentation which is ‘quasi-democratic’ (i.e. quasi-local in energy) and which provides an energy transfer from the source to the medium at a rate (the energy flux \mathcal{F}) which is quasi-independent of ω . The locality of the branching process implies a spectrum of the Kolmogorov-Obukhov type, i.e. a power-law spectrum which is a fixed point of the branching process and whose strength is proportional to the energy flux: $D(\omega) \sim \mathcal{F}/\sqrt{\omega}$ for $\omega \ll \omega_c$. Via this turbulent flow, the gluon cascade loses towards the medium an energy $\Delta E \sim \alpha_s^2 \omega_c$, which is independent of the initial energy E of the leading particle and of the details of the thermalization mechanism at the low-energy end of the cascade. This energy is carried away by very soft gluons, which propagate at very large angles with respect to the jet axis. Our predictions for the value of ΔE and for its angular distribution appear to agree quite well, qualitatively and even semi-quantitatively, with the phenomenology of di-jet asymmetry in nucleus-nucleus collisions at the LHC.

KEYWORDS: Perturbative QCD. Heavy Ion Collisions. Jet quenching. Wave turbulence

Contents

1	Introduction	1
2	Typical scales and physical regimes	5
3	The low–energy regime	7
3.1	The rate equation	7
3.2	The spectrum and the flow energy	9
3.3	Energy flux, turbulence, and thermalization	12
4	The high–energy regime	15
4.1	The coupled rate equations	15
4.2	The radiation spectrum	18
4.3	The energy flux	22
4.4	The energy flux revisited: democratic branchings	26
5	Physical discussion: energy loss at large angles	30
A	Perturbation theory for the rate equation	36

1 Introduction

The experimental observation of the phenomenon known as ‘di–jet asymmetry’ in Pb+Pb collisions at the LHC [1–8] has triggered intense theoretical efforts [9–21] aiming at understanding the evolution of an energetic jet propagating through a dense QCD medium, such as a quark–gluon plasma. The crucial observation is that the part of the jet fragmentation which is triggered by interactions inside the medium is controlled by relatively soft gluon emissions, with energies ω well below the characteristic medium scale $\omega_c = \hat{q}L^2/2$ and a formation time $t_{\text{br}}(\omega)$ much smaller than L . (Here, \hat{q} is the jet quenching parameter, L is the distance travelled by the ‘leading particle’ — the energetic parton which has initiated the jet — through the medium, and the ‘formation time’ $t_{\text{br}}(\omega) \sim \sqrt{\omega/\hat{q}}$ is the typical duration of the branching process.) This observation has far reaching consequences:

The soft gluons can be easily deviated towards large angles by rescattering in the medium, so their abundant production via jet fragmentation may explain the significant transport of energy at large angles with respect to the jet axis — the hallmark of di–jet asymmetry. Also, the subsequent emissions of soft gluons can be viewed as independent from each other and hence described as a classical, probabilistic, branching process. Indeed, the quantum coherence effects and the associated interference phenomena are efficiently washed out by rescattering in the medium [9–11]: the loss of color coherence occurs on a time scale comparable to that of the branching process, so that gluons that emerge from a splitting propagate independently of each other [14].

Based on such considerations, one has been able to derive a classical effective theory for the gluon cascade generated via successive medium–induced gluon branchings [16, 17] (see also Refs. [22, 23] for

earlier, related, studies). This is a stochastic theory for a Markovian process in which the branching rate is given by the BDMPSZ spectrum [24–28] for a single, medium-induced, gluon emission. The branching probability corresponding to a distance L is parametrically of order $\bar{\alpha}[L/t_{\text{br}}(\omega)]$, with $\bar{\alpha} \equiv \alpha_s N_c/\pi$. This probability becomes of order one (meaning that the branching dynamics becomes non-perturbative) when $\omega \lesssim \omega_s \equiv \bar{\alpha}^2 \omega_c$. As we shall see, this ‘soft’ scale ω_s is truly semi-hard (in the ballpark of a few GeV), meaning that there is a significant region in phase-space where perturbation theory breaks down. The effective theory put forward in Refs. [16, 17] allows one to deal with such non-perturbative aspects, by resumming soft multiple branchings to all orders.

The original analysis in [16] demonstrated that the non-perturbative dynamics associated with multiple branchings has a remarkable consequence: it leads to *wave turbulence* [29, 30]. The leading particle, whose initial energy E is typically much larger than the non-perturbative scale ω_s , promptly and abundantly radiates soft gluons with energies $\omega \lesssim \omega_s$ and thus loses an amount of energy of order $\Delta E \sim \omega_s$ *event by event* (that is, with probability of order one). After being emitted, these soft primary gluons keep on branching into even softer gluons, and their subsequent branchings are *quasi-democratic*: the two daughter gluons produced by a typical splitting have comparable energies¹. The locality of the branchings in ω is the key ingredient for turbulence. It leads to a power-law spectrum $D(\omega) \propto 1/\sqrt{\omega}$, which emerges as the Kolmogorov–Zakharov (KZ) fixed point [29, 30] of the branching process (this KZ spectrum is formally similar to the BDMPSZ spectrum), and to an energy flux which is independent of ω — the *turbulent flow*. An energy flux which is uniform in ω means that the energy flows from the high-energy end to the low-energy end of the cascade, without accumulating at any intermediate value of ω . For an ideal cascade, where the branching law remains unchanged down to arbitrary small values of ω , the energy carried by the flow accumulates into a condensate at $\omega = 0$. In practice, we expect the branching process to be modified when the gluon energies become comparable to the medium ‘temperature’ T (the typical energy of the medium constituents): the soft gluons with $\omega \sim T$ ‘thermalize’, meaning that they transfer their energy towards the medium. Assuming the medium to act as a perfect sink at $\omega \simeq T$, we conclude that the rate for energy loss is fixed by the turbulent flow and thus independent of the details of the thermalization mechanism (‘universality’).

An essential property of the turbulent flow is the fact that it allows for the *transfer of a significant fraction of the total energy towards arbitrarily soft quanta*. To better appreciate how non-trivial this situation is, let us compare it with a more traditional parton cascade in perturbative QCD: the DGLAP cascade, as driven by bremsstrahlung in the vacuum. In that case, the typical splittings are very asymmetric, due to the ‘infrared’ ($\omega \rightarrow 0$) singularity of bremsstrahlung, and lead to a rapid rise in the number of gluons with small values of the energy fraction $x \equiv \omega/E$. Yet, the total energy carried by these ‘wee’ gluons with $x \ll 1$ is very small: the energy fraction contained in the region of the spectrum at $x < x_0$ vanishes as a power of x_0 when $x_0 \rightarrow 0$. Most of the original energy remains in the few partons with larger values of x . This is due to the fact that, after a very asymmetric splitting, the parent parton preserves most of its original energy.

By contrast, for the medium-induced cascade, the energy contained in the bins of the spectrum at $x < x_0$ is only a *part* of the total energy associated with modes softer than x_0 . The other part is the energy carried by the turbulent flow, which ends up at arbitrarily low values of x (at least, for an

¹It is interesting to notice that a similar branching process occurs in a different physical context, namely the thermalization of the quark–gluon plasma produced in the intermediate stages of a ultrarelativistic heavy ion collision: during the late stages of the ‘bottom-up’ scenario [22], the hard particles lose energy towards the surrounding thermal bath via soft radiation giving rise to quasi-democratic cascades [31].

ideal cascade) and hence is independent of x_0 . Depending upon the size L of the medium, this flow energy can be as large as the original energy E of the leading particle (see the discussion in Sect. 2). In the presence of a thermalization mechanism at $\omega \sim T$, the above argument remains valid so long as $x_0 \geq x_{\text{th}}$, with $x_{\text{th}} \equiv T/E$. In practice, this ‘thermal’ value $x_{\text{th}} \sim 10^{-2}$ is quite small, so most of the energy lost by the gluon cascade towards the medium is associated with the turbulent flow, and *not* with the (BDMPSZ-like) gluon spectrum². Without this flow, there would be no significant energy transfer towards very small $x \sim x_{\text{th}}$.

Soft gluons propagate at large angles θ with respect to the jet axis: $\theta \sim k_{\perp}/\omega$, where k_{\perp} is the typical transverse momentum acquired by the gluon via rescattering in the medium, and is at most weakly dependent upon ω . So, the ability of the medium-induced cascade to abundantly produce soft gluons provides a natural explanation for the main feature of di-jet asymmetry: the fact that the energy difference between the trigger jet and the away jet is carried by many soft ($p_T \lesssim 2$ GeV) hadrons propagating at large angles ($\theta \gtrsim 0.8$) with respect to the axis of the away jet [2]. This qualitative explanation has been originally proposed in [16] and further developed in Refs. [17–20]. However, these previous studies were not fully conclusive, as they did not explicitly consider the kinematical regime which is pertinent for di-jet asymmetry. Namely, they focused on the ‘low-energy’ regime where the energy E of the leading particle (LP) is smaller than the medium scale ω_c . Albeit the value of ω_c is not precisely known from first principles, its current phenomenological estimates are well below the energy $E \gtrsim 100$ GeV of the trigger jet in the experimental measurements of di-jet asymmetry (see the discussion in Sect. 2). It is our main objective in this paper to provide a thorough analysis of the high-energy regime at $E \gg \omega_c$, including its implications for the phenomenology.

In order to describe our results below, it is useful to recall the physical meaning of the medium scale $\omega_c = \hat{q}L^2/2$: this is the highest possible energy of a medium-induced emission by a parton with energy $E > \omega_c$ which crosses the medium over a distance L . The emission of a gluon with energy ω_c has a formation time $t_{\text{br}}(\omega_c) = L$ and hence a small probability $\bar{\alpha}[L/t_{\text{br}}(\omega_c)] \sim \bar{\alpha}$: this is a *rare* event. Still, such rare but hard emissions dominate the *average* energy loss by the LP, estimated as $\langle \Delta E \rangle \sim \bar{\alpha}\omega_c$ [24–27]. Hence, a very energetic particle with $E \gg \omega_c$ loses only a small fraction $\bar{\alpha}(\omega_c/E) \ll 1$ of its original energy and thus emerges from the medium with an energy $E' \sim E$, which is much larger than the maximal energy ω_c of its radiation. Accordingly, the spectrum shows a *gap* between a peak at $\omega \sim E$, which represents the LP, and a continuum at $\omega \leq \omega_c$, which describes the radiation. The detailed structure of the peak is irrelevant for studies of the di-jet asymmetry: the energy carried by the LP is very closely collimated around the jet axis, within a small angle³ $\theta_{\text{LP}} \sim Q_L/E \ll 1$, which is much smaller than the angular opening of the experimental ‘jet’. This is in agreement with the experimental observation [1, 2] that the azimuthal distribution of di-jets in Pb+Pb collisions is as narrowly peaked at $\Delta\phi = \pi$ as the corresponding distribution in p+p collisions.

In view of the above, our subsequent analysis will focus on the radiation part of the spectrum at $x \leq x_c$, where $x = \omega/E$ and $x_c = \omega_c/E \ll 1$. This part includes the essential physics of multiple branching leading to energy loss via many soft particles propagating at large angles. For the purposes of this analysis, the LP can be treated as a steady source of radiation for gluons with energy fractions

²Incidentally, this explains why earlier studies of the energy distribution based on the BDMPSZ spectrum alone, which have not included the effects of multiple branchings, concluded that there should be very little energy in the gluon cascade at small x and large angles [32], and thus failed to predict the phenomenon of di-jet asymmetry.

³Here, $Q_L^2 \equiv \hat{q}L$ is the transverse momentum broadening acquired by the LP while crossing the medium over a distance L . Some typical values are $Q_L = 2$ GeV, $E = 100$ GeV, and hence $\theta_{\text{LP}} \sim 0.02$.

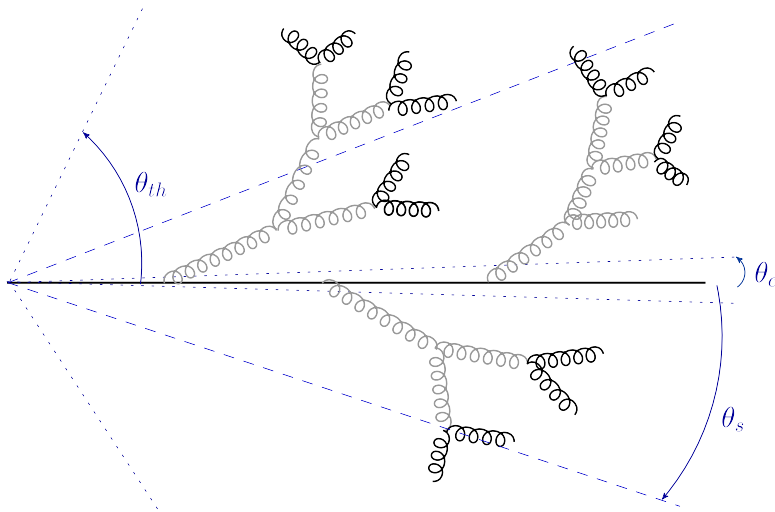


Figure 1. A typical gluon cascade as generated via medium-induced gluon branchings. The small angle $\theta_c \simeq Q_L/\omega_c$ is the propagation angle for a relatively hard gluon with energy $\omega \sim \omega_c$. Such a hard emission is a rare event and hence is not included in our typical event. All the shown gluons (besides the LP) have soft energies $\omega \lesssim \omega_s = \bar{\alpha}^2 \omega_c$, hence their emissions occur with probability of $\mathcal{O}(1)$. The primary gluons are emitted (by the LP) at a typical angle $\theta_s = \theta_c/\bar{\alpha}^2$ and subsequently disappear via branching into even softer gluons. The opaque lines refer to gluons which exist at intermediate stages of the cascade, while the black lines refer to the ‘final’ gluons, which thermalize and propagate at even larger angles, $\theta \sim \theta_{\text{th}} \gg \theta_s$ (see Sect. 5 for details).

$x \leq x_c$. For this effective problem with a source, we will be able to construct exact solutions for the gluon spectrum $D(x, t)$ at any time $t \leq L$, and also for the energy flux $\mathcal{F}(x, t)$ (the rate for energy transfer through the cascade; see Sect. 3 for a precise definition). This energy flux, and more precisely its ‘flow’ limit $\mathcal{F}_{\text{flow}}(t) \equiv \mathcal{F}(x = 0, t)$, is the most interesting quantity in the present context, since it controls the energy transfer by the gluon cascade to the medium.

A non-zero ‘flow’ component in the energy flux is the main signature of turbulence [29, 30] (e.g., there is no such a component for the DGLAP cascade). An important property of turbulence, which follows from the locality of the branchings, is the fact that, within the ‘inertial range’ deeply between the ‘source’ and the ‘sink’, the spectrum is fully determined by the energy flux together with the KZ scaling law. For the standard turbulence in 3+1 dimensions, this relation is known as the ‘Kolmogorov–Obukhov spectrum’. For our present problem in 1+1 dimensions (energy and time), the ‘source’ is the leading particle, the ‘sink’ is the thermal bath, and the ‘inertial range’ correspond to $x_{\text{th}} \ll x \ll 1$. *A priori*, our problem differs from the familiar turbulence set-up via its explicit time-dependence: the source acts only up to a finite time $t_{\text{max}} = L$, which moreover is quite small, in the sense that $\hat{q}L^2 \ll E$. Notwithstanding, we shall demonstrate that a time-dependent generalization of the Kolmogorov–Obukhov relation holds for the problem at hand: the gluon spectrum at $x \ll x_c$ is fully determined by the flow component of the energy flux, together with the characteristic scaling behavior of the BDMPST spectrum (the KZ scaling for the present problem). Namely, we shall find $D(x, t) \propto \mathcal{F}_{\text{flow}}(t)/\sqrt{x}$, where the proportionality constant is under control.

The energy transferred by the gluon cascade to the medium can be identified with the energy ΔE_{flow} carried away by the flow, i.e. the time integral of $\mathcal{F}_{\text{flow}}(t)$ between $t = 0$ and $t = L$. For the high-energy regime under consideration, this quantity turns out to be independent of the original

energy E of the LP and to have a transparent physical interpretation⁴: $\Delta E_{\text{flow}} \simeq v \omega_s$, where $\omega_s = \bar{\alpha}^2 \omega_c$ and $v \simeq 4.96$ is a pure number which can be interpreted as the average number of soft primary emissions with energies $\omega \sim \omega_s$. Such soft gluons are radiated by the LP with probability of order one and they subsequently transfer their energy towards the medium via successive, quasi-democratic, branchings. A typical gluon cascade is illustrated in Fig. 1. Using phenomenologically motivated values for \hat{q} and L , we find $\Delta E_{\text{flow}} \simeq 10 \div 20$ GeV (see Sect. 5). Since carried by very soft gluons, with energies $\omega \sim T \ll \omega_s$, this energy propagates at very large angles with respect to the jet axis, at least as large as $\theta_s \equiv Q_L/\omega_s \sim 0.5$. (θ_s is the typical propagation angle of the soft primary gluons, and its above estimate will be discussed in Sect. 5.) By progressively increasing the jet opening angle θ_0 within a rather wide range, say from $\theta_0 \sim \theta_s$ up to $\theta_0 \sim 1$, we can recover part of the missing energy, *but only very slowly*: most of this energy lies at even larger angles, $\theta \sim \theta_{\text{th}} \gg \theta_s$ (see Fig. 1 and Sect. 5 for details). The above predictions — the numerical estimate for the energy loss at large angles ΔE_{flow} and its extremely weak dependence upon the jet opening angle θ_0 — are in good agreement, qualitative and even semi-quantitative, with the phenomenology of di-jet asymmetry at the LHC [2, 4, 5, 8]. Vice versa, we believe that these particular LHC data could not be understood in a scenario which neglects multiple branchings, nor in one which uses a vacuum-like model for the in-medium gluon fragmentation, that is, a model which ignores the quasi-democratic nature of the soft branchings and the associated turbulent flow.

Our paper is organized as follows. In Sect. 2 we shall introduce, via qualitative considerations and parametric estimates, the main physical scales which control the medium-induced gluon branching and allow one to separate between various physical regimes. In Sect. 3, we shall consider the low-energy regime at $E \lesssim \omega_c$ as a warm-up. Besides a succinct review of the main results obtained in Ref. [16], this section will also contain some new material, like the explicit calculation of the energy flux and a first discussion of the Kolmogorov–Obukhov relation. Sects. 4 and 5 will be devoted to the main new problem of interest for us here: the high-energy regime at $E \gg \omega_c$. Sect. 4 will present the main theoretical developments: the justification of the effective problem with a source, the exact, analytic and numerical, solutions for the radiation spectrum at $\omega \leq \omega_c$ and for the turbulent flow, the democratic nature of the branchings and its physical implications, and the proof of the (time-dependent version of the) Kolmogorov–Obukhov relation for the branching dynamics at hand. Finally, in Sect. 5 we shall discuss some phenomenological consequences of this dynamics for the energy lost by the jet via soft gluons propagating at large angles.

2 Typical scales and physical regimes

We would like to study the gluon cascade generated via successive medium-induced gluon branchings by an original gluon — the ‘leading particle’ (LP) — with energy E which propagates through a dense QCD medium along a distance L . For the present purposes, the medium is solely characterized by a transport coefficient \hat{q} , known as the ‘jet quenching parameter’, which measures the dispersion in transverse momentum acquired by a parton propagating through this medium per unit length (or time). Depending upon its energy, the leading particle can either escape the medium, or disappear inside it (in the sense of not being distinguishable from its products of fragmentation). The actual scenario depends upon the ratio between E and a characteristic medium scale $\omega_c \equiv \hat{q}L^2/2$, which is the maximal energy of a gluon whose emission can be triggered by multiple scattering in the medium:

⁴This estimate for ΔE_{flow} holds to leading order in $\bar{\alpha}$; see Eq. (5.4) and the plots in Sect. 5 for more accurate results.

gluons with an energy $\omega \sim \omega_c$ have a formation time of order L and an emission probability of order $\bar{\alpha} \equiv \alpha_s N_c / \pi$. Another energy scale that will play an important role in what follows is the *soft* scale $\omega_s \equiv \bar{\alpha}^2 \omega_c$: gluons with $\omega \sim \omega_s$ have a relatively short formation time $t_{\text{br}}(\omega) \sim \bar{\alpha} L$ and an emission probability of order 1. This scale is ‘soft’ since $\omega_s \ll \omega_c$ at weak coupling and since one generally has $E \gg \omega_s$ in the applications to phenomenology (see below).

More generally, the elementary probability $\Delta\mathcal{P}$ for a gluon with energy ω to be radiated (via the BDMPSZ mechanism) during a time interval Δt can be parametrically estimated as

$$\Delta\mathcal{P} \sim \bar{\alpha} \frac{\Delta t}{t_{\text{br}}(\omega)} \sim \bar{\alpha} \sqrt{\frac{\hat{q}}{2\omega}} \Delta t, \quad (2.1)$$

where $t_{\text{br}}(\omega) \simeq \sqrt{2\omega/\hat{q}}$ is the ‘gluon formation time’ — more precisely, the typical duration of a branching process in which the softest of the two daughter gluons has an energy $\omega \ll \omega_c$. Eq. (2.1) holds so long as $\Delta\mathcal{P} \ll 1$. When $\Delta\mathcal{P} \sim \mathcal{O}(1)$, the multiple branchings become important and the evolution of the gluon cascade becomes non-perturbative (in the sense that the effects of multiple branchings must be resummed to all orders). As clear from Eq. (2.1), for any $\Delta t < L$, there exists a sufficiently soft sector where the branching dynamics is non-perturbative: this occurs at $\omega \lesssim \omega_s(\Delta t) \equiv \bar{\alpha}^2 \hat{q} \Delta t^2 / 2$. In particular, for $\Delta t = L$, this yields back the ‘soft’ scale aforementioned: $\omega_s(L) = \omega_s$.

The above discussion in particular implies that the quantity ω_s sets the scale for the energy lost by the LP in a *typical event*: with a probability of $\mathcal{O}(1)$, the LP particle emits primary gluons with energies of $\mathcal{O}(\omega_s)$, and thus loses an energy $\Delta E \sim \omega_s$. Accordingly, the *typical* energy loss, as measured event-by-event, is sensitive to multiple branchings. On the other hand, the *average* energy loss $\langle \Delta E \rangle$ is dominated by rare but hard emissions, with energies $\omega \gg \omega_s$, for which the effects of multiple branchings are negligible. One finds indeed

$$\langle \Delta E \rangle \simeq \int^{\omega_{\text{max}}} d\omega \omega \frac{dN}{d\omega} \simeq \bar{\alpha} \int^{\omega_{\text{max}}} d\omega \sqrt{\frac{\omega_c}{\omega}} \sim \bar{\alpha} \sqrt{\omega_c \omega_{\text{max}}}, \quad (2.2)$$

where the gluon spectrum $\omega(dN/d\omega)$ is essentially the elementary probability for a single branching, Eq. (2.1), evaluated for $\Delta t = L$ and the upper limit $\omega_{\text{max}} \equiv \min(\omega_c, E)$ is typically much larger than ω_s . The integral in Eq. (2.2) is dominated by its upper limit, i.e. by energies $\omega \sim \omega_{\text{max}} \gg \omega_s$.

The global features of the medium-induced gluon cascade depend upon the relative values of these three scales E , ω_c , and ω_s . Namely, for a given medium scale ω_c , one can distinguish between three interesting physical regimes, depending upon the energy E of the leading particle: (i) *high energy* $E \gg \omega_c$, (ii) *intermediate energy* $\omega_c \gtrsim E \gg \omega_s$, and (iii) *low energy* $E \lesssim \omega_s$. Recalling that $\omega_c = \hat{q} L^2 / 2$, we see that the ‘high energy’ regime can also be viewed as the limit where the in-medium path L is relatively small, whereas the ‘low energy’ case corresponds to relatively large values of L .

In case (i), both the average energy loss $\langle \Delta E \rangle \sim \bar{\alpha} \omega_c$ and its typical value $\Delta E \sim \omega_s$ are much smaller than E , and the probability to find the LP outside the (already narrow) energy interval $(E - \omega_c, E)$ is negligibly small. Accordingly, in this case there is a *gap in the spectrum* between a ‘peak’ at $\omega \simeq E$ representing the leading particle and a ‘continuum’ at $\omega \lesssim \omega_c$ representing the radiated gluons.

In case (ii), the typical energy loss is still much smaller than E , so the leading particle survives in most of the events, yet there is a sizable fraction of the events, of $\mathcal{O}(\bar{\alpha})$ or larger, where both fragmentation products carry similar energies. Accordingly, the LP peak is visible in the spectrum,

but there is no gap anymore. The average energy loss $\langle \Delta E \rangle \sim \bar{\alpha} \sqrt{\omega_c E}$ is still smaller than the original energy E , but it represents a relatively large fraction of it, of order $\gtrsim \bar{\alpha}$.

In case (iii), both the typical and the average energy loss are of order E , meaning that the LP undergoes strong fragmentation and ‘disappears’ in most, if not all, of the events. Of course, this should be also the faith of the very soft ($\omega \lesssim \omega_s$) gluons produced via radiation in cases (i) and (ii). So, in this third case, the spectrum contains no peak or other structure suggestive of the LP.

To summarize, the first two cases have in common the fact that the LP survives after crossing the medium, but they differ in the actual shape of the spectrum (with or without a gap). The last two cases are both characterized by the absence of a gap, but they differ in the fact that the LP peak is still visible in case (ii), whereas it is totally washed out in case (iii).

To make contact with the phenomenology, we chose $\hat{q} = 1 \text{ GeV}^2/\text{fm}$ (a reasonable estimate for a weakly coupled quark–gluon plasma [24] which moreover appears to be consistent with recent analyses of data [33]), $\bar{\alpha} = 0.3$, and let L vary from 2 to 6 fm. For the three particular values $L = (2, 4, 6) \text{ fm}$, we deduce $\omega_c \simeq (10, 40, 90) \text{ GeV}$ and $\omega_s \simeq (1, 4, 9) \text{ GeV}$. Hence, when one is interested in the phenomenology of high–energy jets with $E \geq 100 \text{ GeV}$, as in the studies of di–jet asymmetry at the LHC, one should mainly consider the case (i) above. On the other hand, for studies of the nuclear modification factor R_{AA} , where the energies of the measured hadrons vary from 1 GeV to about 20 GeV, one is mostly in the situations covered by cases (ii) and (iii). These last two cases have been thoroughly discussed in the recent literature, in particular in relation with the disappearance of the leading particle and the energy transport at large angles [16–20], but to our knowledge the first case has not been studied in detail so far. From the previous discussion, it should be clear that this is the most relevant case for a study of di–jet asymmetry in Pb+Pb collisions at the LHC. This is the main problem that we would like to address in what follows.

3 The low–energy regime

In preparation for the discussion of the high–energy regime at $E \gg \omega_c$, it is useful to first review some known results concerning the low and intermediate regimes at $E \lesssim \omega_c$ [16, 17] (see also Refs. [22, 23, 34] for earlier, related, studies). These two regimes can be simultaneously discussed, as they refer to different limits of a same theoretical description.

3.1 The rate equation

Throughout this paper we shall focus on the gluon spectrum integrated over transverse momenta, i.e.

$$D(\omega, t) \equiv \omega \frac{dN}{d\omega} = \int d^2\mathbf{k} \omega \frac{dN}{d\omega d^2\mathbf{k}}, \quad (3.1)$$

where $\omega \leq E$ and \mathbf{k} denote the energy and respectively transverse momentum of a gluon in the cascade, N is the number of gluons, and it is understood that the evolution time obeys $0 \leq t \leq L$. The function $D(\omega, t)$ describes the energy distribution within the cascade and its evolution with time. For sufficiently soft gluons at least, namely so long as $\omega \ll \omega_c$, and to leading order⁵ in α_s , this

⁵A class of particularly large radiative corrections, which are enhanced by the double–logarithm $\ln^2(LT)$, can be effectively resummed into the effective dynamics by replacing the ‘bare’ value of the jet quenching parameter \hat{q} by its renormalized value, as recently computed in Refs. [35–39].

evolution can be described as a classical stochastic branching process [14, 16, 17], with the elementary splitting rate determined by the BDMPSZ spectrum [24–28]. Specifically, the differential probability per unit time and per unit z for a gluon with energy ω to split into two gluons with energy fractions respectively z and $1 - z$ is

$$\frac{d^2 \mathcal{P}_{\text{br}}}{dz dt} = \frac{\alpha_s}{2\pi} \frac{P_{g \rightarrow g}(z)}{t_{\text{br}}(z, \omega)}, \quad (3.2)$$

where $P_{g \rightarrow g}(z) = N_c [1 - z(1 - z)]^2 / z(1 - z)$, with $0 < z < 1$, is the leading order gluon–gluon splitting function, N_c is the number of colors, and $t_{\text{br}}(z, \omega)$ is the typical duration of the branching process:

$$t_{\text{br}}(z, \omega) \equiv \sqrt{\frac{z(1 - z)\omega}{\hat{q}_{\text{eff}}(z)}}, \quad \hat{q}_{\text{eff}}(z) \equiv \hat{q} [1 - z(1 - z)]. \quad (3.3)$$

Note that this branching time depends upon both the energy ω of the parent gluon and the splitting fraction z , and that it is much smaller than L whenever at least one of the two daughter particles, with energies $z\omega$ and respectively $(1 - z)\omega$, is soft compared to ω_c .

The elementary splitting rate (3.2) together with the requirement of probability conservation completely specifies the structure of the stochastic branching process and, in particular, the evolution equation obeyed by the gluon spectrum. So long as $E < \omega_c$, this equation reads

$$\frac{\partial D(x, \tau)}{\partial \tau} = \bar{\alpha} \int dz \mathcal{K}(z) \left[\sqrt{\frac{z}{x}} D\left(\frac{x}{z}, \tau\right) - \frac{z}{\sqrt{x}} D(x, \tau) \right], \quad (3.4)$$

in convenient notations where $D(x, \tau) \equiv D(\omega, t)$, $x \equiv \omega/E \leq 1$ is the energy fraction with respect to the leading particle, and

$$\tau \equiv \sqrt{\frac{\hat{q}}{E}} t = \sqrt{2x_c} \frac{t}{L}, \quad x_c \equiv \frac{\omega_c}{E}, \quad (3.5)$$

is the reduced time (the evolution time in dimensionless units). Notice that $x_c > 1$ for the physical problems discussed in this section. The splitting kernel $\mathcal{K}(z)$ is defined as

$$\mathcal{K}(z) \equiv \frac{f(z)}{[z(1 - z)]^{3/2}} = \mathcal{K}(1 - z), \quad f(z) \equiv [1 - z(1 - z)]^{5/2}. \quad (3.6)$$

It depends only upon the splitting fraction z since the corresponding dependence upon the energy (fraction) x of the leading particle, cf. Eq. (3.2), has been explicitly factored out in writing Eq. (3.4).

We shall refer to the r.h.s. of Eq. (3.4) as the ‘branching term’ and denote it as $\bar{\alpha} \mathcal{I}[D]$. This is the sum of two terms, which can be recognized as the familiar ‘gain’ and ‘loss’ terms characteristic of a branching process. The first term, which is positive and nonlocal in x , is the *gain term*: it describes the rise in the number of gluons at x due to emissions from gluons at larger $x' = x/z$. The respective integral over z is restricted to $x < z < 1$ by the support of $D(x/z, \tau)$. The second, negative, term, which is local in x , represents the *loss term* and describes the reduction in the number of gluons at x due to their decay into gluons with smaller $x' = zx$. Taken separately, the gain term and the loss term in Eq. (3.4) have endpoint singularities at $z = 1$, but these singularities exactly cancel between the two terms and the overall equation is well defined.

As anticipated, Eq. (3.4) encompasses the two regimes at ‘low’ and ‘intermediate’ energies introduced in Sect. 2. In fact, there is no fundamental difference between the dynamics in these two regimes,

rather they differ only in the maximal value for the reduced time τ which is allowed in practice. This maximal value, namely $\tau_L \equiv \sqrt{2x_c} = \sqrt{\hat{q}/E} L$, increases with the medium size L , but decreases with the energy E of the leading particle. In the ‘intermediate energy’ regime, the evolution is limited to relatively small times, $1 \lesssim \tau_L \ll 1/\bar{\alpha}$, whereas in the ‘low energy’ one, it can extend up to much larger values: $\tau_L \gtrsim 1/\bar{\alpha}$. This explains the qualitative differences between the two regimes that were anticipated in Sect. 2 and will be now demonstrated via explicit solutions to Eq. (3.4).

3.2 The spectrum and the flow energy

To study the effects of multiple branchings, one needs a non-perturbative solution to Eq. (3.4). Whereas it is straightforward to solve this equation via numerical methods, for the purpose of demonstrating subtle physical phenomena, it is much more convenient to dispose of an analytic solution. Such a solution has been obtained in Ref. [16], but for the simplified kernel $\mathcal{K}_0(z) \equiv 1/[z(1-z)]^{3/2}$, which is obtained from Eq. (3.6) after replacing the slowly varying factor $f(z)$ in the numerator by 1. This simplified kernel has the same singularities at $z = 0$ and $z = 1$ as the original kernel $\mathcal{K}(z)$, hence it is expected to have similar physical implications, at least qualitatively. (This will also be checked via numerical simulations later on; see e.g. Fig. 4.)

For the simplified kernel $\mathcal{K}_0(z)$ and the initial condition $D(x, \tau = 0) = \delta(x - 1)$, corresponding to a single gluon (the ‘leading particle’) carrying all the energy at $\tau = 0$, the exact solution reads [16]

$$D(x, \tau) = \frac{\bar{\alpha}\tau}{\sqrt{x}(1-x)^{3/2}} \exp\left\{-\frac{\pi\bar{\alpha}^2\tau^2}{1-x}\right\}. \quad (3.7)$$

This is recognized as the product between the BDMPSZ spectrum [24–28] (which is the same as the result of the first iteration of Eq. (3.4)),

$$D_0(x, \tau) = \frac{\bar{\alpha}\tau}{\sqrt{x}(1-x)^{3/2}}, \quad (3.8)$$

and a Gaussian factor describing, at early times, the broadening of the peak associated with the LP [40] and, at late times, the suppression of the spectrum as whole.

To be more specific, consider increasing the time from $\tau = 0$ up to the maximal value $\tau_L = \sqrt{2x_c}$, where we recall that $x_c > 1$. When $\tau \rightarrow 0$, the r.h.s. of Eq. (3.7) approaches $\delta(x - 1)$, as it should. So long as τ is small enough for $\pi\bar{\alpha}^2\tau^2 \ll 1$, the spectrum exhibits a pronounced peak in the vicinity of $x = 1$, which describes the leading particle: the maximum of this peak lies at x_p with $1 - x_p \simeq (2\pi/3)\bar{\alpha}^2\tau^2$ and its width Δx around x_p is of order $\pi\bar{\alpha}^2\tau^2$. The fact that the peak gets displaced below 1 is a consequence of the Gaussian factor in Eq. (3.7), which strongly suppresses the spectrum for x close to 1, within a window

$$1 - x \lesssim \pi\bar{\alpha}^2\tau^2 \ll 1. \quad (3.9)$$

The physical origin of this suppression should be clear in view of the discussion in Sect. 2: for x close to 1, the quantity $\epsilon \equiv (1-x)E$ is the energy lost by the leading particle via radiation. Eq. (3.9) shows that the typical value of this energy is $\epsilon(t) \simeq 2\pi\omega_s(t)$, with $\omega_s(t) = \bar{\alpha}^2\hat{q}t^2/2$ the non-perturbative scale for the onset of multiple branching, as introduced in Sect. 2. That is, the LP copiously radiates very soft gluons, for which the emission probability is of $\mathcal{O}(1)$, and thus loses an energy of order $\omega_s(t)$. Interestingly, this energy loss is enhanced by the relatively large numerical factor 2π , which can be

interpreted as the average number of gluons with energy $\omega \sim \omega_s(t)$ that are emitted by the LP during a time interval t . This interpretation will be supported by other findings below.

Let us now increase τ towards larger values $\pi\bar{\alpha}^2\tau^2 \gtrsim 1$. This is of course possible only in the ‘low energy’ regime where $\tau_L \gtrsim 1/\bar{\alpha}$. Then the Gaussian suppression extends to all values of x , the LP peak gets washed out — it broadens, it moves towards smaller values of x , and its height is decreasing — and eventually disappears from the spectrum. One can say that a LP with energy $E \lesssim \bar{\alpha}^2\omega_c$ has a finite ‘lifetime’ inside the medium, of order $\Delta\tau \sim 1/\bar{\alpha}$ or, in physical units (cf. Eq. (3.5)),

$$\Delta t \sim \frac{1}{\bar{\alpha}} \sqrt{\frac{E}{\hat{q}}}. \quad (3.10)$$

More precisely, this means that the LP has fragmented into gluons which carry a sizable fraction of its original energy E . Via successive branchings, the energy gets degraded to lower and lower values of x , and it is interesting to understand this evolution in more detail. A priori, one might expect this energy to accumulate in the small- x part of the spectrum, and notably at $x \lesssim x_s(\tau) \equiv \bar{\alpha}^2\tau^2$ (corresponding to $\omega \lesssim \omega_s(t)$), but Eq. (3.7) shows that this is actually *not* the case: for $x \ll 1$, Eq. (3.7) reduces to

$$D(x, \tau) \simeq \frac{\bar{\alpha}\tau}{\sqrt{x}} e^{-\pi\bar{\alpha}^2\tau^2}, \quad (3.11)$$

which has exactly the same shape in x as the small- x limit of the BDMPSZ spectrum, Eq. (3.8). In fact, Eq. (3.11) formally looks like the BDMPSZ spectrum produced via a single emission by the LP, times a Gaussian factor describing the decay of the LP with increasing time. This interpretation seems to imply that multiple branchings are not important at small x , but from the discussion in Sect. 2 we know that this cannot be true: after a time t , the single-branching probability becomes of order one (meaning that multiple branching becomes important) for all the soft modes obeying $x < x_s(\tau)$. This last condition can also be inferred from Eq. (3.8): when $x \sim x_s(\tau) \ll 1$, the BDMPSZ spectrum becomes of $\mathcal{O}(1)$.

We are thus facing an apparent paradox — in spite of the importance of multiple branching, the energy does not get accumulated in the bins of the spectrum at small x — which finds its solution in the phenomenon of *wave turbulence* [16]. The BDMPSZ spectrum at small x is not modified by the fragmentation because this represents a *fixed point* of the rate equation (3.4) at small $x \ll 1$: the branching term vanishes (meaning that the ‘gain’ and ‘loss’ terms compensate each other) when evaluated with the ‘scaling’ spectrum $D_{\text{sc}}(x) \equiv 1/\sqrt{x}$. This can be recognized as the Kolmogorov–Zakharov (KZ) spectrum [29, 30] for the branching process at hand. In turn, the existence of this fixed point implies that, via successive branchings, the energy gets transmitted from large x to small x , without accumulating at any intermediate value of x : it rather flows throughout the spectrum and accumulates into a condensate at $x = 0$.

This is illustrated in Fig. 2, where the exact solution (3.7) is represented as a function of x for several values of τ , up to relatively large values, such that $\pi\bar{\alpha}^2\tau^2 \gtrsim 1$. The early-time set of curves, at $\tau \lesssim 1$, where the LP peak is still visible, is representative for the ‘intermediate energy’ regime, where the late-time curves, from which the LP has disappeared and where the spectrum is seen to be suppressed as a whole, correspond to the ‘low energy’ case.

The energy flow can also be studied analytically, on the basis of Eq. (3.7). To that aim, consider the energy balance between spectrum and flow. The energy fraction contained in the spectrum after

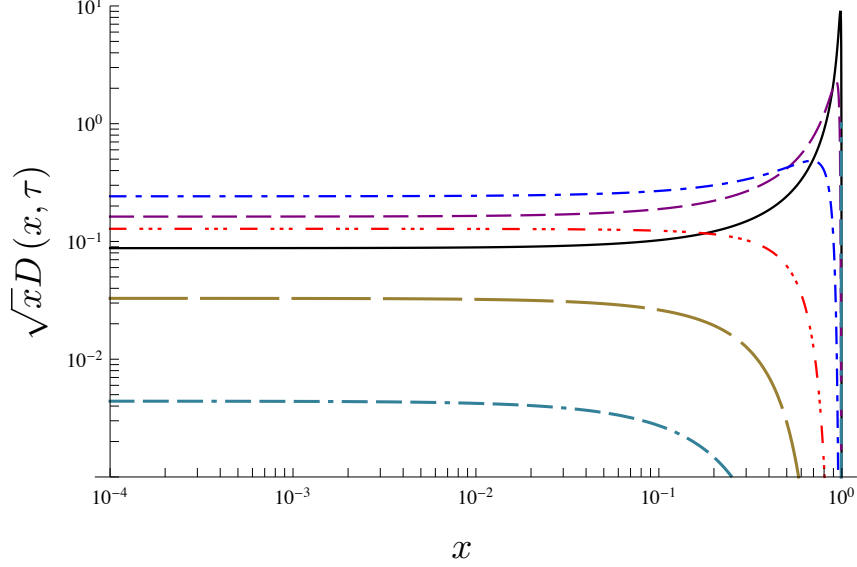


Figure 2. Plot (in log-log scale) of $\sqrt{x}D(x, \tau)$, with $D(x, \tau)$ given by Eq. (3.7), as a function of x for various values of τ : solid (black): $\tau = 0.3$; dashed (purple): $\tau = 0.6$; dashed-dotted (blue): $\tau = 1.3$; dashed-triple dotted (red): $\tau = 2.5$; long-dashed (brown): $\tau = 3.5$; triple dashed-dotted (green): $\tau = 4.5$. We use $\bar{\alpha} = 0.3$.

a time τ is computed as [16]

$$\mathcal{E}(\tau) = \int_0^1 dx D(x, \tau) = e^{-\pi\bar{\alpha}^2\tau^2}, \quad (3.12)$$

and decreases with time. The difference

$$\mathcal{E}_{\text{flow}}(\tau) \equiv 1 - \mathcal{E}(\tau) = 1 - e^{-\pi\bar{\alpha}^2\tau^2}, \quad (3.13)$$

is the energy fraction carried by the flow, i.e. by the multiple branchings, and which formally ends up in a condensate at $x = 0$. For sufficiently large times $\bar{\alpha}\tau \gtrsim 1$ (corresponding to the low-energy regime), this can be as large as the total initial energy of the LP.

It is also interesting to consider the small time limit of Eq. (3.13), that is

$$\mathcal{E}_{\text{flow}}(\tau) \simeq \pi\bar{\alpha}^2\tau^2 = 2\pi x_s(\tau) \quad \text{for} \quad \pi\bar{\alpha}^2\tau^2 \ll 1. \quad (3.14)$$

This result can be interpreted as follows: $\nu_0 \equiv 2\pi$ is the average number of primary gluons with energies of the order of $\omega_s(t) = \bar{\alpha}^2\hat{q}t^2/2$ that are emitted by the leading particle during a time t . This number is independent of t or $\bar{\alpha}$, since such gluon emissions occur with probability of order one. Stated differently, the typical time interval between two successive such emissions is of order t . [This interval can be estimated from the condition that $\Delta\mathcal{P} \sim \mathcal{O}(1)$, with $\Delta\mathcal{P}$ given by Eq. (2.1) with $\omega \sim \omega_s(t)$; this implies $\Delta t \sim (1/\bar{\alpha})t_{\text{br}}(\omega_s(t)) \simeq t$.] After being emitted, these soft primary gluons rapidly cascade into even softer gluons and thus eventually transmit (after a time $\Delta t \sim t$ estimated as above) their whole energy to the arbitrarily soft quanta which compose the flow. This argument also shows that the gluons with energies $\omega \sim \omega_s(t)$ not only are emitted with a probability of $\mathcal{O}(1)$ during an interval of order t , but also have a ‘lifetime’ $\Delta t \sim t$ before they branch again with probability of $\mathcal{O}(1)$.

3.3 Energy flux, turbulence, and thermalization

The physical interpretation of Eq. (3.13) in terms of multiple branchings and, in particular, its relation to turbulent flow become more transparent if one studies a more differential quantity, the *energy flux* $\mathcal{F}(x_0, \tau)$. This is defined as the rate for energy transfer from the region $x > x_0$ to the region $x < x_0$. Since the energy in the region $x > x_0$ is decreasing with time, via branchings, it is natural to define the flux as the following, positive, quantity

$$\mathcal{F}(x_0, \tau) \equiv -\frac{\partial \mathcal{E}^>(x_0, \tau)}{\partial \tau} = \frac{\partial \mathcal{E}^<(x_0, \tau)}{\partial \tau}, \quad (3.15)$$

where $\mathcal{E}^>(x_0, \tau)$ is the energy fraction contained in the bins of the spectrum with $x > x_0$, that is,

$$\mathcal{E}^>(x_0, \tau) = \int_{x_0}^1 dx D(x, \tau), \quad (3.16)$$

whereas the complementary quantity $\mathcal{E}^<(x_0, \tau)$ is the energy fraction carried by the modes with $x < x_0$. In turn, $\mathcal{E}^<(x_0, \tau)$ is the sum of two contributions : the flow energy (3.13) and the energy contained in the bins of the spectrum at $x < x_0$; that is,

$$\mathcal{E}^<(x_0, \tau) = 1 - \mathcal{E}^>(x_0, \tau) = \mathcal{E}_{\text{flow}}(\tau) + \int_0^{x_0} dx D(x, \tau). \quad (3.17)$$

Using the above definitions together with Eq. (3.7) for $D(x, \tau)$, it is straightforward to numerically compute the energy flux $\mathcal{F}(x_0, \tau)$, with the results displayed in Fig. 3. For a physical discussion, it is convenient to focus on the behavior at small $x_0 \ll 1$. In that region, one can use Eq. (3.17) together with the small- x approximation to the spectrum, Eq. (3.11), to deduce the analytic estimate

$$\mathcal{F}(x_0, \tau) \simeq \left[2\pi\bar{\alpha}^2\tau + 2\bar{\alpha}\sqrt{x_0}(1 - 2\pi\bar{\alpha}^2\tau^2) \right] e^{-\pi\bar{\alpha}^2\tau^2}. \quad (3.18)$$

The first term within the square brackets, which is independent of x_0 , is the flow contribution,

$$\mathcal{F}_{\text{flow}}(\tau) \equiv \frac{\partial \mathcal{E}_{\text{flow}}(\tau)}{\partial \tau} = 2\pi\bar{\alpha}^2\tau e^{-\pi\bar{\alpha}^2\tau^2}, \quad (3.19)$$

while the second term, proportional to $\sqrt{x_0}$, is the rate at which the energy changes in the region of the spectrum at $x \leq x_0$. Clearly, the flow component in Eq. (3.19) dominates over the non-flow one at sufficiently small values of x_0 , such that $x_0 \lesssim x_s(\tau) = \bar{\alpha}^2\tau^2$. This is also visible in Fig. 3, where the various curves become indeed flat at sufficiently small x_0 .

We thus see that the small- x behavior of the flux, and unlike the corresponding behavior of the spectrum, does reveal the non-perturbative nature of the multiple branchings and of the associated scale x_s : in the soft region at $x_0 \lesssim x_s(\tau)$, the flux $\mathcal{F}(x_0, \tau)$ is controlled by its ‘flow’ component and is quasi-independent of x_0 . A *uniform* energy flux is the distinguished signature of (wave) turbulence [29, 30]. It physically means that the energy flows through the spectrum without accumulating at intermediate values of x . To see this, let us compute the rate of change for $\mathcal{E}(x_1, x_2, \tau)$ — the energy fraction contained within the interval $x_1 < x < x_2$:

$$\mathcal{E}(x_1, x_2, \tau) = \int_{x_1}^{x_2} dx D(x, \tau) \implies \frac{\partial \mathcal{E}(x_1, x_2, \tau)}{\partial \tau} = \mathcal{F}(x_2, \tau) - \mathcal{F}(x_1, \tau). \quad (3.20)$$

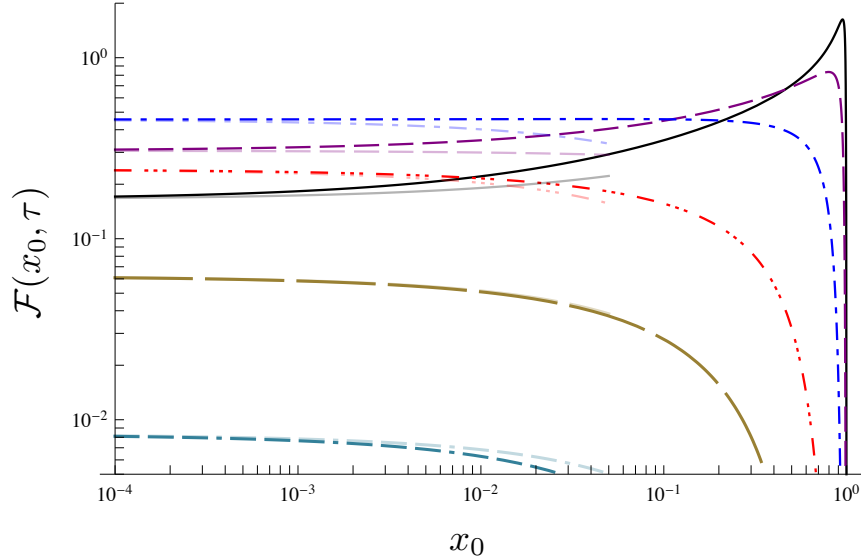


Figure 3. Plot (in log-log scale) of the energy flux $\mathcal{F}(x_0, \tau)$, cf. Eq. (3.15), as a function of x_0 for various values of τ . We use the same conventions as in Fig. 2. The thin curves, which are drawn for $x_0 \leq 0.05$, represent the approximation in Eq. (3.18), which is valid at small x_0 .

This rate vanishes if the flux is independent of x . In our case, the flux is not strictly uniform, not even at very small values of x (see Eq. (3.18)). Yet, the energy flux which crosses a bin at $x \lesssim x_s(\tau)$ is much larger than the rate for energy change in that bin: the energy flows through the bin, without accumulating there.

It is intuitively clear that a quasi-uniform flux requires the branchings to be *quasi-local* in x (or ‘quasi-democratic’). Since, if the typical branchings were strongly asymmetric, then after each branching most of the energy would remain in the parent gluon and the energy would accumulate in the bins at large x . It is also quite clear, in view of the general arguments in Sect. 2, that in the non-perturbative region at $x \lesssim x_s(\tau)$ the branchings are indeed quasi-local: a gluon with energy $x \sim x_s(\tau)$ splits with probability of $\mathcal{O}(1)$ during a time interval τ *irrespective of the value z of the splitting fraction*. Hence, there is no reason why special values like $z \ll 1$ or $1 - z \ll 1$ should be favored. A more elaborate argument in favor of democratic branchings will be presented in Sect. 4.4.

The locality of the interactions is a fundamental property of turbulence [29, 30]. In the traditional turbulence problem, where the energy is injected by a time-independent source which is localized in energy and produces a steady spectrum, this property ensures that the energy spectrum in the ‘inertial range’ (i.e. sufficiently far away from the source) can be expressed in terms of the (steady) flux \mathcal{F} and a special power-like spectrum, the ‘Kolmogorov–Zakharov spectrum’, which is a fixed-point of the ‘collision term’. In the case of hydrodynamic turbulence in 3+1 dimensions, this relation between the energy spectrum and the flux is known as the ‘Kolmogorov–Obukhov spectrum’.

For the problem at hand, where the ‘source’ is the leading particle originally localized at $x = 1$, the ‘inertial region’ corresponds to $x \ll 1$, the ‘collision term’ term is the branching term $\bar{\alpha}\mathcal{I}[D]$, and the fixed-point solution is the scaling spectrum $D_{sc}(x) = 1/\sqrt{x}$. But unlike for the more conventional

set-up, our current problem is clearly *not* stationary: the ‘source’ (the LP) loses energy and can even disappear at large times, so both the spectrum and the energy flux have non-trivial time dependencies. Notwithstanding, it turns out that the fundamental relation alluded to above, between the energy spectrum and the flux, also holds for the time-dependent physical problem at hand. Namely, by inspection of Eqs. (3.11) and (3.19), it is clear than one can write

$$D(x, \tau) \simeq \frac{1}{2\pi\bar{\alpha}} \frac{\mathcal{F}_{\text{flow}}(\tau)}{\sqrt{x}} \quad \text{for } x \ll 1. \quad (3.21)$$

This relation can be recognized as a version of the celebrated Kolmogorov–Obukhov scaling adapted to the current problem and generalized to a time-dependent situation. Note that Eq. (3.21) involves only the flow contribution to the flux, albeit this relation holds for any $x \ll 1$ and not only in the ‘non-perturbative’ sector at $x \lesssim x_s(\tau)$. At this level, the relation (3.21) might look fortuitous, but in Sect. 4.4 we shall present a general argument showing that it has a deep physical motivation.

So far, we have implicitly assumed that the branching dynamics as described by Eq. (3.4) extends all the way down to $x = 0$, that is, it includes arbitrarily soft gluons. In reality, the dynamics should change at sufficiently low energies, for various reasons. First, when the gluons in the cascade become as soft as the medium constituents — that is, their energies become comparable to the temperature T — they rapidly thermalize via collisions in the medium and thus ‘disappear’ from the cascade. Second, the BDMPSZ branching law (3.2) assumes the dominance of multiple soft scattering and hence it ceases to be valid when the branching time $t_{\text{br}}(z, \omega)$ becomes as low as the mean free path ℓ between successive collisions in the medium. This condition restricts the gluon energies to values $\omega \gtrsim \omega_{\text{BH}} \equiv \hat{q}\ell^2/2$. For a weakly coupled quark–gluon plasma, the ‘Beithe–Heitler’ scale ω_{BH} is comparable to the temperature T . (Indeed, in this case, one has $\hat{q} \sim \bar{\alpha}^2 T^3$ and $\ell \sim (\bar{\alpha}T)^{-1}$ to parametric accuracy.) With this example in mind, we shall not distinguish between these two scales anymore, but simply assume that the dynamics described by Eq. (3.4) applies for all the energies $\omega \gtrsim T$, i.e., for all $x \gtrsim x_{\text{th}} \equiv T/E$. In all the interesting problems, the thermal scale x_{th} is small enough to allow for multiple branchings: $x_{\text{th}} \ll x_s = \bar{\alpha}^2 x_c$. For instance, in the case of a weakly coupled plasma, the above condition is tantamount to $L \gg \ell/\bar{\alpha} \sim (\bar{\alpha}^2 T)^{-1}$, which is indeed satisfied since the interesting values for L are much larger than the typical relaxation time $\lambda_{\text{rel}} \sim (\bar{\alpha}^2 T)^{-1}$ of the plasma.

Notice that we implicitly assume here that the thermalization mechanism acts as a ‘perfect sink’ at $x \sim x_{\text{th}}$. (A similar assumption was made e.g. in the ‘bottom-up’ scenario for thermalization [22].) That is, the surrounding medium absorbs the energy from the cascade at a rate equal to the relevant flux $\mathcal{F}(x_{\text{th}}, \tau)$, without modifying the branching dynamics at higher values $x \gg x_{\text{th}}$. This is a rather standard assumption in the context of turbulence and is well motivated for the problem at hand, as we argue now. To that aim, one should compare the relaxation time $\lambda_{\text{rel}} \sim (\bar{\alpha}^2 T)^{-1}$ aforementioned, which represents the characteristic thermalization time at weak coupling, with the lifetime $\Delta t(\omega)$ of a gluon generation (the time interval between two successive branchings) for gluons with energy $\omega \sim T$, which is the characteristic time scale for the turbulent flow. This $\Delta t(\omega)$ can be estimated as explained at the end of Sect. 3.2, and reads (to parametric accuracy)

$$\Delta t(\omega) \sim \frac{1}{\bar{\alpha}} t_{\text{br}}(\omega) \sim \frac{1}{\bar{\alpha}} \sqrt{\frac{\omega}{\hat{q}}}. \quad (3.22)$$

Using $\omega \sim T$ and the perturbative estimate $\hat{q} \sim \bar{\alpha}^2 T^3$, one deduces $\Delta t(T) \sim (\bar{\alpha}^2 T)^{-1} \sim \lambda_{\text{rel}}$. We thus conclude that the physics of thermalization is as efficient in dissipating the energy as the turbulent flow. This implies that there should be no energy pile-up towards the low-energy end of the cascade.

Under these assumptions, it is interesting to compute the total energy lost by the cascade towards the medium, i.e. ‘the energy which thermalizes’. This is the same as the energy which has crossed the bin x_{th} during the overall time τ_L , namely (cf. Eq. (3.17))

$$\mathcal{E}_{\text{th}} \equiv \mathcal{E}^<(x_{\text{th}}, \tau_L) \simeq 1 - e^{-\pi\bar{\alpha}^2\tau_L^2} + 2\bar{\alpha}\tau_L\sqrt{x_{\text{th}}}e^{-\pi\bar{\alpha}^2\tau_L^2}, \quad (3.23)$$

where the approximate equality holds since $x_{\text{th}} \ll 1$. Eq. (3.23) is recognized as the sum of the flow energy, Eq. (3.13), and of the energy that would be contained in the spectrum at $x \leq x_{\text{th}}$, cf. Eq. (3.11). Using $\tau_L = \sqrt{2x_c}$ and $x_{\text{th}} \ll x_s = \bar{\alpha}^2x_c$, it is easy to check that the flow component dominates over the spectrum piece, and hence $\mathcal{E}_{\text{th}} \simeq \mathcal{E}_{\text{flow}}(\tau_L)$. This implies that the energy lost by the gluon cascade towards the medium is independent of the details of the thermalization process, like the precise value of x_{th} . This universality too is a well known feature of a turbulent process [29, 30].

4 The high-energy regime

With this section, we begin the study of the main physical problem of interest for us in this paper, namely the gluon cascade produced in the medium by a very energetic leading particle, with original energy $E \gg \omega_c$. The main new ingredient as compared to the previous discussion is a kinematical restriction on the primary gluon emissions that can be triggered by interactions in the medium: the energy ω of the gluons emitted by the LP cannot exceed a value ω_c in order for the respective formation times to remain smaller than L . When $x_c \equiv \omega_c/E \ll 1$, this restriction has important consequences: it implies that the LP loses only a small fraction of its total energy, of order $\bar{\alpha}x_c \ll 1$. Our main focus in what follows will not be on this average energy lost by the LP (this is well understood within the original BDMPST formalism, including multiple soft emissions of primary gluons [40]), but rather on the further evolution of this radiation via multiple branchings and the associated flow of energy towards small values of x and large angles.

4.1 The coupled rate equations

Since the radiation is restricted to relatively low energies $\omega \leq \omega_c \ll E$, or $x \leq x_c \ll 1$, it is clear that the part of the spectrum at higher energies $x_c < x < 1$ has to be associated with the LP. This makes it natural to decompose the overall spectrum as

$$D(x, \tau) = [\Theta(x - x_c) + \Theta(x_c - x)]D(x, \tau) \equiv D_{\text{LP}}(x, \tau) + D_{\text{rad}}(x, \tau). \quad (4.1)$$

In reality, the LP piece $D_{\text{LP}}(x, \tau)$ is a rather narrow peak located in the vicinity of $x = 1$ (see below), so there is a large gap between the two components of the spectrum.

The evolution of the radiation via successive branchings involves no special constraint, so the respective rate equation can be obtained simply by replacing $D(x, \tau)$ according to Eq. (4.1) in the r.h.s. of the general equation Eq. (3.4) (restricted to $x < x_c$, of course). This yields

$$\frac{\partial D_{\text{rad}}(x, \tau)}{\partial \tau} = \mathcal{S}(x, \tau) + \bar{\alpha} \int dz \mathcal{K}(z) \left\{ \sqrt{\frac{z}{x}} D_{\text{rad}}\left(\frac{x}{z}, \tau\right) - \frac{z}{\sqrt{x}} D_{\text{rad}}(x, \tau) \right\}, \quad (4.2)$$

where the *source* $\mathcal{S}(x, \tau)$ is the energy per unit time and per unit x radiated by the LP:

$$\mathcal{S}(x, \tau) \equiv \bar{\alpha} \int dz \mathcal{K}(z) \sqrt{\frac{z}{x}} D_{\text{LP}}\left(\frac{x}{z}, \tau\right). \quad (4.3)$$

It is here implicitly understood that this source has support at $x \leq x_c$ and that it acts over a limited interval in time, at $0 \leq \tau \leq \tau_L \equiv \sqrt{2x_c}$, which is moreover small, $\tau_L \ll 1$, in the high-energy regime of interest. The integral over z in the gain term of Eq. (4.2) is restricted to $x/x_c < z < 1$, where the lower limit is introduced by the support of the function $D_{\text{rad}}(x/z, \tau)$.

In the rate equation for the leading particle, one needs to enforce the condition that the radiated gluons have energy fractions smaller than x_c . The ensuing equation reads (with $x > x_c$)

$$\begin{aligned} \frac{\partial D_{\text{LP}}(x, \tau)}{\partial \tau} = \bar{\alpha} \int dz \mathcal{K}(z) \left\{ \Theta \left(z - \frac{x}{x+x_c} \right) \sqrt{\frac{z}{x}} D_{\text{LP}} \left(\frac{x}{z}, \tau \right) \right. \\ \left. - \frac{z}{\sqrt{x}} D_{\text{LP}}(x, \tau) \left[\Theta \left(z - 1 + \frac{x_c}{x} \right) + \Theta \left(\frac{x_c}{x} - z \right) \right] \right\} \end{aligned} \quad (4.4)$$

where the various Θ -functions enforce the kinematical constraint: In the gain term, one requires that the unmeasured gluon emitted (with splitting fraction $1-z$) by the LP (with initial energy fraction x/z) be softer than x_c : $(1-z)(x/z) < x_c \implies z > x/(x+x_c)$. In the loss term, one requires that one of the daughter gluons be soft: either $zx < x_c$, or $(1-z)x < x_c$.

As it should be clear from the previous discussion, the functions $D_{\text{LP}}(x, \tau)$ and $D_{\text{rad}}(x, \tau)$ at any time $\tau < \tau_L$ also depend upon x_c , hence upon the overall size L of the medium, via the kinematical constraints on the gluon emissions. This shows that the dynamics in this high energy regime is *non-local in time*; e.g., the branching rate in Eq. (4.4) ‘knows’ about the maximal time τ_L via the various Θ -functions, which involve x_c . This property reflects a true non-locality of the underlying quantum dynamics: it takes some time to emit a gluon and this time cannot be larger than L . Accordingly, at any $\tau < \tau_L$, one should only initiate emissions whose energies are smaller than ω_c : gluon fluctuations with higher energies would have no time to become on-shell. The kinematical constraint $\omega \leq \omega_c$ reflects only in a crude way the actual non-locality of the quantum emissions. The classical description at hand, as based on rate equations, is truly appropriate only for the sufficiently soft emissions with small formation times $t_{\text{br}}(\omega) \ll L$. Fortunately, these are the most important emissions for the physics problems that we shall here address.

In the zeroth order approximation, which is strictly valid as $\tau \rightarrow 0$, one can use $D_{\text{LP}}(x, \tau) = \delta(1-x)$, and then the source in Eq. (4.3) reduces to the BDMPSZ spectrum, as expected:

$$\mathcal{S}_0(x) \equiv \bar{\alpha} x \mathcal{K}(x) \simeq \frac{\bar{\alpha}}{\sqrt{x}}. \quad (4.5)$$

In writing the second, approximate, equality we have used the fact that x is small, $x \leq x_c \ll 1$, to simplify the expression of the splitting kernel (cf. Eq. (3.6)): $\mathcal{K}(x) \simeq x^{-3/2}$ for $x \ll 1$.

We shall now argue that the expression (4.5), which is time-independent, remains a good approximation for all the times τ of interest. Of course, the spectrum $D_{\text{LP}}(x, \tau)$ of the LP changes quite fast with increasing τ , notably due to the prompt radiation of very soft quanta with energy fractions $x \lesssim x_s(\tau) = \bar{\alpha}^2 \tau^2$. This leads to a broadening of the LP peak on the scale $\Delta x \sim \bar{\alpha}^2 \tau^2 \lesssim \bar{\alpha}^2 x_c \ll 1$, similar to that exhibited by Eq. (3.7) at small times. Yet, the probability to emit a relatively hard gluon with $x \sim x_c$ is very small, of $\mathcal{O}(\bar{\alpha})$. Accordingly, the support of the function $D_{\text{LP}}(x, \tau)$ remains limited to a narrow band at $1-x_c \lesssim x < 1$, which is well separated from the radiation spectrum at $x < x_c$. Hence, the integration over z in Eq. (4.3) is effectively restricted to a narrow range close to x , namely $x < z < x/(1-x_c)$, and the integral can be approximated as

$$\mathcal{S}(x, \tau) \simeq \bar{\alpha} x \mathcal{K}(x) \int dx' D_{\text{LP}}(x', \tau) \simeq \frac{\bar{\alpha}}{\sqrt{x}} \left[1 + \mathcal{O}(x, \bar{\alpha} x_c) \right]. \quad (4.6)$$

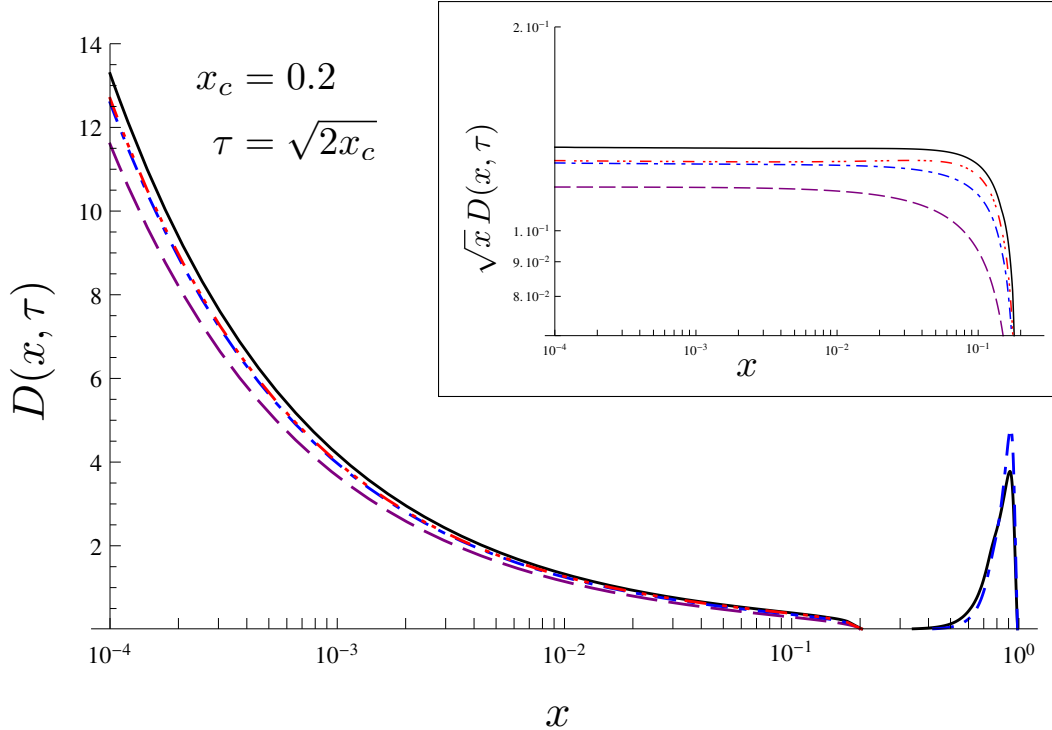


Figure 4. The full spectrum $D(x, \tau) = D_{\text{LP}}(x, \tau) + D_{\text{rad}}(x, \tau)$ obtained by numerically solving the coupled equations (4.2) and (4.4), versus the radiation spectrum predicted by Eq. (4.8) with a source. We use both versions of the kernel, \mathcal{K} and \mathcal{K}_0 , together with $x_c = 0.2$ and $\tau = \sqrt{2x_c} \simeq 0.63$. (i) Simplified kernel \mathcal{K}_0 : black curve: Eqs. (4.2)–(4.4); purple, dashed: Eq. (4.8). (ii) Full kernel \mathcal{K} : blue, dashed–dotted: Eqs. (4.2)–(4.4); red, dashed–triple dotted: Eq. (4.8). In the insert: the same plots (for the radiation part only) in log–log scale.

Here we have used the fact that the overall strength of the function $D_{\text{LP}}(x, \tau)$, i.e. the energy fraction carried by the LP after a time τ , can be estimated as

$$\mathcal{E}_{\text{LP}}(\tau) \equiv \int dx D_{\text{LP}}(x, \tau) \simeq 1 - 2\bar{\alpha}\tau\sqrt{x_c}, \quad (4.7)$$

that is, the initial energy minus the energy lost via radiation of soft gluons with $x \leq x_c$, cf. Eq. (4.5).

To summarize, after an evolution time τ_L , the energetic LP loses only a small fraction $\bar{\alpha}\sqrt{x_c}\tau_L \sim \bar{\alpha}x_c \ll 1$ of its total energy and its spectral density remains peaked near $x = 1$. Accordingly, it can be effectively treated as a steady source $\mathcal{S}_0(x)$ for the soft radiation at $x \ll 1$. This is verified in the plots in Fig. 4, where we perform two types of comparisons: (i) between the evolution with the exact kernel \mathcal{K} in Eq. (3.6) and that with the simplified kernel \mathcal{K}_0 , and (ii) between the solution to the coupled system of equations (4.2) and (4.4) and that to the effective equation with a source, i.e. Eq. (4.2) with $\mathcal{S}(x, \tau) \rightarrow \mathcal{S}_0(x)$. As one can see in this plot, the two choices for the kernel lead indeed to results which are qualitatively similar and numerically very close to each other. Furthermore, the radiation spectrum at $x \leq x_c$ produced by the ‘model’ equation with a source is indeed close to the respective prediction of the coupled rate equations. (In fact, for the exact kernel \mathcal{K} , this similarity looks even more striking — the respective curves almost overlap with each other at sufficiently small

x — but in our opinion this is merely a coincidence.) In the next subsection, we shall construct an exact analytic solution for the equation with the source, for the case of the simplified kernel \mathcal{K}_0 .

4.2 The radiation spectrum

In the remaining part of this section, we shall concentrate on the solution to the following equation

$$\begin{aligned} \frac{\partial D_{\text{rad}}(x, \tau)}{\partial \tau} &= \frac{\bar{\alpha}}{\sqrt{x}} + \bar{\alpha} \int dz \mathcal{K}(z) \left\{ \sqrt{\frac{z}{x}} D_{\text{rad}}\left(\frac{x}{z}, \tau\right) - \frac{z}{\sqrt{x}} D_{\text{rad}}(x, \tau) \right\} \\ &\equiv \mathcal{S}_0(x) + \bar{\alpha} \mathcal{I}[D_{\text{rad}}](x, \tau), \end{aligned} \quad (4.8)$$

which, as above argued, offers a good approximation for the dynamics of the medium-induced radiation by a leading particle with high energy $E \gg \omega_c$. This is an inhomogeneous equation with vanishing initial condition and can be solved with the help of the respective Green's function:

$$D_{\text{rad}}(x, \tau) = \int_x^{x_c} dx_1 \int_0^\tau d\tau_1 G(x, x_1, \tau - \tau_1) \mathcal{S}_0(x_1). \quad (4.9)$$

The Green's function $G(x, x_1, \tau)$ obeys the homogeneous version of Eq. (4.8) with initial condition $G(x, x_1, \tau) = \delta(x - x_1)$.

From now on, we shall again restrict ourselves to the case of the simplified splitting kernel $\mathcal{K}_0(z)$, which we recall is obtained by replacing $f(z) \rightarrow 1$ in Eq. (3.6). For this case, the Green's function $G(x, x_1, \tau)$ can be exactly computed, since it is closely related to the function $D(x, \tau)$ in Eq. (4.10): both functions obey Eq. (3.4), but with slightly different initial conditions. It is easy to check that the corresponding solutions are related via an appropriate rescaling of the variables:

$$G(x, x_1, \tau) = \frac{1}{x_1} D\left(\frac{x}{x_1}, \frac{\tau}{\sqrt{x_1}}\right) = \sqrt{\frac{x_1}{x}} \frac{\bar{\alpha}\tau}{(x_1 - x)^{3/2}} \exp\left\{-\frac{\pi\bar{\alpha}^2\tau^2}{x_1 - x}\right\}. \quad (4.10)$$

Since the source $\mathcal{S}_0(x_1)$ in Eq. (4.9) is independent of time, the integral over τ_1 involves only the Green's function and can be readily computed:

$$\int_0^\tau d\tau_1 G(x, x_1, \tau - \tau_1) = \frac{1}{2\pi\bar{\alpha}} \sqrt{\frac{x_1}{x(x_1 - x)}} \left[1 - \exp\left\{-\frac{\pi\bar{\alpha}^2\tau^2}{x_1 - x}\right\}\right]. \quad (4.11)$$

To also compute the integral over x_1 , it is convenient to change the integration variable according to $u \equiv \pi\bar{\alpha}^2\tau^2/(x_1 - x)$. One thus easily finds

$$D_{\text{rad}}(x, \tau) = \frac{\bar{\alpha}\tau}{\sqrt{x}} \frac{1}{2\sqrt{\pi}} \int_\zeta^\infty \frac{du}{u^{3/2}} [1 - e^{-u}] = \frac{\bar{\alpha}\tau}{\sqrt{x}} \left\{ \frac{1}{\sqrt{\pi}} \Gamma\left(\frac{1}{2}, \zeta\right) + \frac{1 - e^{-\zeta}}{\sqrt{\pi\zeta}} \right\}, \quad (4.12)$$

where

$$\zeta \equiv \zeta(x_c - x, \tau) \equiv \frac{\pi\bar{\alpha}^2\tau^2}{x_c - x}, \quad (4.13)$$

and

$$\Gamma\left(\frac{1}{2}, \zeta\right) \equiv \int_\zeta^\infty \frac{dz}{\sqrt{z}} e^{-z} = \sqrt{\pi} - \int_0^\zeta \frac{dz}{\sqrt{z}} e^{-z} = \sqrt{\pi} - \gamma\left(\frac{1}{2}, \zeta\right), \quad (4.14)$$

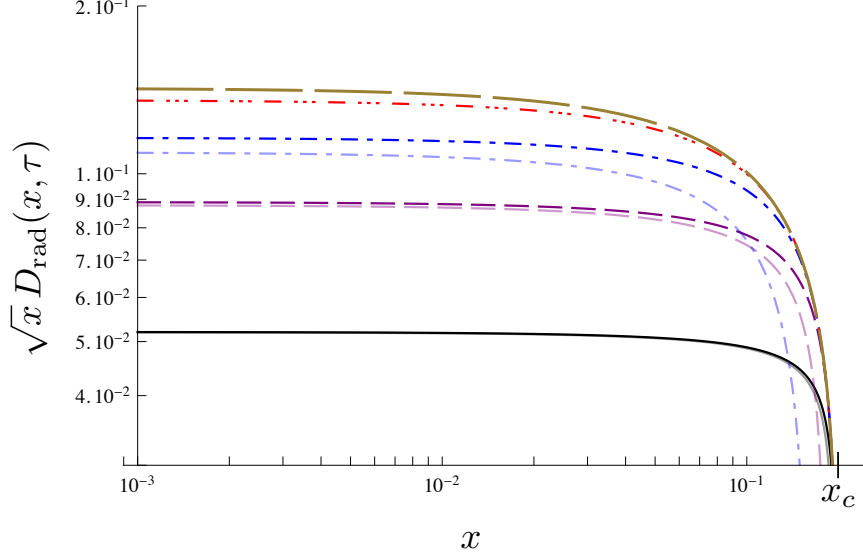


Figure 5. Plot (in log-log scale) of $D_{\text{rad}}(x, \tau)$, cf. Eq. (4.12), as a function of x for $x_c = 0.2$ and various values of τ . The thick curves show the function $\sqrt{x}D_{\text{rad}}(x, \tau)$ for $\tau = 0.2$ (black, solid), $\tau = 0.4$ (purple, dashed), $\tau = 0.63$ (blue, dashed–dotted), and $\tau = 1.0$ (red, dashed–triple dotted). Note that the maximal value for τ which is physically allowed is $\tau_L = \sqrt{0.4} \simeq 0.63$. The thin curves, shown for $\tau \leq \tau_L$, represent the corresponding approximations at small $\zeta(x_c - x, \tau)$, as obtained by keeping only the first 2 terms in the Taylor expansion in Eq. (4.20). The enveloping curve (brown, long–dashed) is the limiting curve at large ζ , cf. Eq. (4.21).

is the upper incomplete Gamma function (whereas $\gamma(1/2, \zeta)$ is the respective lower function). Note that $D_{\text{rad}}(x, \tau)$ is also a function of the limiting energy fraction x_c , but in our notations this dependence is left implicit. A similar observation applies to all formulæ that appear in this section.

For what follows, it is also useful to single out the piece of the spectrum that would be produced by the source term alone, in the absence of branchings. Specifically, using Eq. (4.14), we can write

$$\begin{aligned}
 D_{\text{rad}}(x, \tau) &= \frac{\bar{\alpha}\tau}{\sqrt{x}} - \delta D_{\text{br}}(x, \tau), \\
 \delta D_{\text{br}}(x, \tau) &\equiv \frac{\bar{\alpha}\tau}{\sqrt{x}} \left\{ \frac{1}{\sqrt{\pi}} \gamma\left(\frac{1}{2}, \zeta\right) - \frac{1 - e^{-\zeta}}{\sqrt{\pi\zeta}} \right\} \equiv \frac{\bar{\alpha}\tau}{\sqrt{x}} h(\zeta),
 \end{aligned}
 \tag{4.15}$$

where the quantity $\delta D_{\text{br}}(x, \tau)$ is the change in the spectrum due to multiple branchings and it is positive semi–definite, as one can easily check — meaning that the effect of branchings is a *depletion* in the spectrum, at any $x \leq x_c$. This depletion reflects the flow of energy from one parton generation to the next one, via parton branching — a phenomenon to which we shall return in the next subsection. But before doing that, let us discuss the radiation spectrum (4.12) in more detail.

This spectrum is depicted in Fig. 5 as a function of x for various values of τ . The different limiting behaviors can be also understood in analytic terms. To that aim, it is useful to notice a few properties of the function $h(\zeta)$. This function is monotonously increasing and interpolates between $h = 0$ at $\zeta = 0$ and $h \rightarrow 1$ as $\zeta \rightarrow \infty$. Furthermore, the ratio $h(\zeta)/\sqrt{\zeta}$ is an analytic function of ζ with infinite

radius of convergence and a rapidly converging Taylor expansion:

$$\sqrt{\frac{\pi}{\zeta}} h(\zeta) = \int_0^1 du u^{-1/2} e^{-\zeta u} - \frac{1 - e^{-\zeta}}{\zeta} = 1 - \frac{1}{6}\zeta + \frac{1}{30}\zeta^2 + \mathcal{O}(\zeta^3). \quad (4.16)$$

Finally, for large ζ , one finds the asymptotic behavior

$$1 - h(\zeta) = \frac{1}{\sqrt{\pi\zeta}} + \dots, \quad (4.17)$$

where the dots stand for terms which are exponentially suppressed.

Returning to the spectrum in Eq. (4.15), we first observe that at small $x \ll x_c$ this reduces to the scaling spectrum $D_{sc}(x) = 1/\sqrt{x}$ — the expected fixed point of the branching dynamics at small x . Indeed, when $x \ll x_c$, one can approximate $\zeta(x_c - x, \tau) \simeq \zeta(x_c, \tau)$ and therefore

$$D_{rad}(x, \tau) \simeq \frac{\bar{\alpha}\tau}{\sqrt{x}} [1 - h(\zeta_0)], \quad \zeta_0 \equiv \zeta(x_c, \tau) = \frac{\pi\bar{\alpha}^2\tau^2}{x_c}. \quad (4.18)$$

Interestingly, at the end of the evolution, i.e. for $\tau = \tau_L = \sqrt{2x_c}$, Eq. (4.18) reduces to the BDMPSZ spectrum times a function of the QCD coupling $\bar{\alpha}$, which is strictly smaller than 1 and which expresses the reduction in the spectrum due to multiple branchings:

$$D_{rad}(x, \tau_L) \simeq \bar{\alpha} \sqrt{\frac{2x_c}{x}} [1 - h(2\pi\bar{\alpha}^2)] \quad \text{for } x \ll x_c. \quad (4.19)$$

Consider now larger values of x , where the deviations from the scaling spectrum start to be important. So long as x is not too close to x_c , such that $\zeta \lesssim 1$, the spectrum can be expanded in powers of ζ , with the help of Eq. (4.16). One thus finds

$$D_{rad}(x, \tau) = \frac{\bar{\alpha}\tau}{\sqrt{x}} \left\{ 1 - \frac{\bar{\alpha}\tau}{\sqrt{x_c - x}} + \frac{\pi}{6} \left(\frac{\bar{\alpha}\tau}{\sqrt{x_c - x}} \right)^3 + \dots \right\} \quad \text{when } \zeta(x_c - x, \tau) \lesssim 1, \quad (4.20)$$

where the dots stand for terms of $\mathcal{O}(\zeta^{5/2})$ and higher. This expansion is rapidly converging for any $\zeta \lesssim 1$. Given that $\zeta(x_c, \tau_L) = 2\pi\bar{\alpha}^2$ is a relatively small number ($2\pi\bar{\alpha}^2 \simeq 0.6$ for $\bar{\alpha} = 0.3$), we expect a limited expansion like Eq. (4.20) to be quite accurate for any $\tau \lesssim \tau_L$ and for x values in the bulk. And indeed, the curves obtained by keeping just the first 2 terms in this expansion provide an excellent approximation to the full curves in Fig. 5 for any $\tau \leq \tau_L$, except of course for x very close to x_c . Notice that the inclusion of the first correction in Eq. (4.20), which expresses the dominant effect of the multiple branchings at small $\bar{\alpha}\tau$, is truly essential in order to obtain such a good agreement. Indeed, for $\tau \sim \tau_L$ and x values in the bulk, that correction is numerically important, of relative order $\bar{\alpha}\tau_L/\sqrt{x_c} = \sqrt{2}\bar{\alpha} \simeq 0.4$.

The expansion in Eq. (4.20) breaks down when the first correction becomes of $\mathcal{O}(1)$ or larger, namely for $x_c - x \lesssim \bar{\alpha}^2\tau^2$. This is in agreement with the fact that the emission of very soft gluons, with energy fractions $x \lesssim x_s(\tau) = \bar{\alpha}^2\tau^2$, is non-perturbative. To investigate the effect of such emissions via analytic approximations, let us consider the behavior near the endpoint of the spectrum, at $x \rightarrow x_c$. In that limit, one has $\zeta \gg 1$, so one can use Eq. (4.17) to deduce

$$D_{rad}(x, \tau) \simeq \frac{1}{\pi} \sqrt{\frac{x_c - x}{x}} \quad \text{when } \zeta(x_c - x, \tau) \gg 1. \quad (4.21)$$

This result is time-independent and shows that the spectrum vanishes when $x \rightarrow x_c$ at any time τ . This demonstrates the efficiency of the soft branchings in depleting the spectrum near its endpoint. The energy which is transferred in this way towards the bins at $x < x_c$ cannot be compensated by a corresponding flow of energy coming from the bins at $x > x_c$, since the spectrum ends at x_c .

The steady spectrum in Eq. (4.21) also represents the limiting curve for the function $D_{\text{rad}}(x, \tau)$ in the formal large-time limit at $\zeta(x_c, \tau) = \pi\bar{\alpha}^2\tau^2/x_c \gg 1$. That is, in this limit, the spectrum takes the form in Eq. (4.21) for *any* $x \leq x_c$. This large-time limit is merely formal, since, as already mentioned, the maximal value for $\zeta(x_c, \tau)$ which is physically allowed is $\zeta(x_c, \tau_L) = 2\pi\bar{\alpha}^2$, which is not that large. Still, this limit is conceptually interesting, in that it corresponds to the more familiar turbulence set-up: a steady situation in which the whole energy injected by the source flows through the spectrum into the ‘sink’ at $x = 0$ (see the discussion in the next subsection).

It is finally interesting to clarify the suitability of perturbation theory (by which we mean the iterative solution to Eq. (4.8) in which the branching term $\bar{\alpha}\mathcal{I}[D_{\text{rad}}]$ is treated as a small perturbation) for the problem at hand. Via successive iterations, one can construct a perturbative solution for $D_{\text{rad}}(x, \tau)$ in the form of a series in powers of $\bar{\alpha}\tau$ and is interesting to compare this series to the small- ζ expansion of the exact solution in Eq. (4.20). Clearly, we do not expect this perturbative approach to be reliable near the endpoint of the spectrum at x_c , but one may hope that it becomes meaningful for x well below x_c and for small times $\bar{\alpha}\tau \ll 1$ — that is, in the region where the expansion (4.20) can be viewed too as a series in powers of $\bar{\alpha}\tau$. But even this last expectation is naive, as shown by following argument: a perturbative solution via iterations would generate both odd and even powers of $\bar{\alpha}\tau$, whereas the corresponding expansion in Eq. (4.20) contains only odd powers.

To further clarify this mismatch, we shall construct in Appendix A the perturbative solution to low orders: $D_{\text{rad}} = D_{\text{rad}}^{(0)} + D_{\text{rad}}^{(1)} + D_{\text{rad}}^{(2)} + \dots$. The zeroth order result is, clearly, $D_{\text{rad}}^{(0)} = \bar{\alpha}\tau/\sqrt{x}$, while the first iteration, as obtained by evaluating the branching term $\bar{\alpha}\mathcal{I}[D_{\text{rad}}]$ with the zeroth order result, yields precisely the correction of $\mathcal{O}(\bar{\alpha}\tau)$ shown in Eq. (4.20), that is,

$$D_{\text{rad}}^{(1)}(x, \tau) = -\frac{\bar{\alpha}^2\tau^2}{\sqrt{x(x_c - x)}}. \quad (4.22)$$

But a subtle issue shows up starting with the second iteration: the first-order correction $D_{\text{rad}}^{(1)}$ turns out to be an *exact fixed point* of the branching kernel: $\mathcal{I}[D_{\text{rad}}^{(1)}] = 0$. Accordingly, the second-order correction is exactly zero, $D_{\text{rad}}^{(2)} = 0$ (still in agreement with Eq. (4.20)), but then the same is true for all the subsequent iterations: $D_{\text{rad}}^{(n)} = 0$ for any $n \geq 2$. That is, the perturbative expansion, as computed without any approximation, terminates after just one non-trivial iteration and predicts $D_{\text{rad}} = D_{\text{rad}}^{(0)} + D_{\text{rad}}^{(1)}$. This prediction is certainly incorrect (except as an approximation at small times and small x): it differs from the actual expansion Eq. (4.20) of the exact result and, in particular, it becomes negative and divergent when $x \rightarrow x_c$.

The mathematical origin of this failure will be clarified in Appendix A. But its physical origin should be quite clear: we have already noticed the non-perturbative nature of the dynamics associated with the emission of very soft quanta, with energy fractions $x \lesssim x_s = \bar{\alpha}^2\tau^2$. For such emissions, the effects of multiple branchings must be resumed to all orders and cannot be accurately studied via iterations. This non-perturbative dynamics is responsible for the rapid broadening of the LP peak and also for the fact that the radiation spectrum in Eq. (4.12) exactly vanishes as $x \rightarrow x_c$ for any τ . Similar, non-perturbative aspects affect the spectrum at any value of x , including the intermediate

bins at $x_s \ll x \ll x_c$, since the occupation of any such a bin can change via the emission of very soft gluons. Hence, not surprisingly, the spectrum $D(x, \tau)$ cannot be faithfully computed within perturbation theory for generic values (x, τ) , albeit interesting information can be obtained via this method in special cases, as we shall see.

4.3 The energy flux

As in Sect. 3, the dissipative properties of the cascade, in particular, the rate for energy loss towards the medium, can be best studied by computing the energy flux associated with branchings. Let $\mathcal{E}(x_0, x_c, \tau)$ denote the energy which at time τ is contained in the modes in the spectrum within the interval $x_0 < x < x_c$:

$$\mathcal{E}(x_0, x_c, \tau) = \int_{x_0}^{x_c} dx D_{\text{rad}}(x, \tau). \quad (4.23)$$

When increasing τ , this energy can change via two mechanisms: (i) it increases due to additional radiation by the source, at a rate $\int_{x_0}^{x_c} dx \mathcal{S}_0(x)$, and (ii) it decreases due to the energy transfer towards the modes at $x < x_0$ via gluon branching, at a rate which is by definition the energy flux $\mathcal{F}(x_0, \tau)$ through the bin x_0 . Hence, we can write

$$\frac{\partial \mathcal{E}(x_0, x_c, \tau)}{\partial \tau} = \int_{x_0}^{x_c} dx \mathcal{S}_0(x) - \mathcal{F}(x_0, \tau), \quad (4.24)$$

which immediately implies

$$\mathcal{F}(x_0, \tau) = \int_{x_0}^{x_c} dx \frac{\partial}{\partial \tau} \delta D_{\text{br}}(x, \tau) = -\bar{\alpha} \int_{x_0}^{x_c} dx \mathcal{I}[D_{\text{rad}}](x, \tau), \quad (4.25)$$

where the first equality follows after recalling the definition (4.15) of $\delta D_{\text{br}}(x, \tau)$, and the second one after also using the rate equation (4.8). Each of the two integral representations for $\mathcal{F}(x_0, \tau)$ in the equation above has its own virtues. When combined with the explicit result for $\delta D_{\text{br}}(x, \tau)$ shown in Eq. (4.15), the first representation allows for efficient numerical calculations, with results that we shall shortly describe. On the other hand, this formula is not well suited for analytic studies, as we shall see. The second integral representation, which involves the branching term $\mathcal{I}[D_{\text{rad}}]$, is more directly connected to the dynamics of branchings and admits a transparent physical interpretation, to be discussed in Sect. 4.4. A priori, this representation seems to be mathematically more involved, in that it involves a double convolution over the spectrum. Yet, as we shall see, this representation allows for more accurate analytic studies. In particular, it will permit us to deduce an exact analytic result in the important limit $x_0 \rightarrow 0$.

Using the first equality in Eq. (4.25) together with the expression (4.15) for $\delta D_{\text{br}}(x, \tau)$, one finds, after simple manipulations,

$$\mathcal{F}(x_0, \tau) = \frac{\bar{\alpha}}{\sqrt{\pi}} \int_{x_0}^{x_c} \frac{dx}{\sqrt{x}} \gamma\left(\frac{1}{2}, \zeta\right), \quad (4.26)$$

with $\zeta \equiv \zeta(x_c - x, \tau)$ as defined in Eq. (4.13). We are mostly interested in the limit $x_0 \rightarrow 0$ of this result, which represents the energy flux carried by the turbulent flow:

$$\mathcal{F}_{\text{flow}}(\tau) = \frac{\bar{\alpha}}{\sqrt{\pi}} \int_0^{x_c} \frac{dx}{\sqrt{x}} \gamma\left(\frac{1}{2}, \zeta\right). \quad (4.27)$$

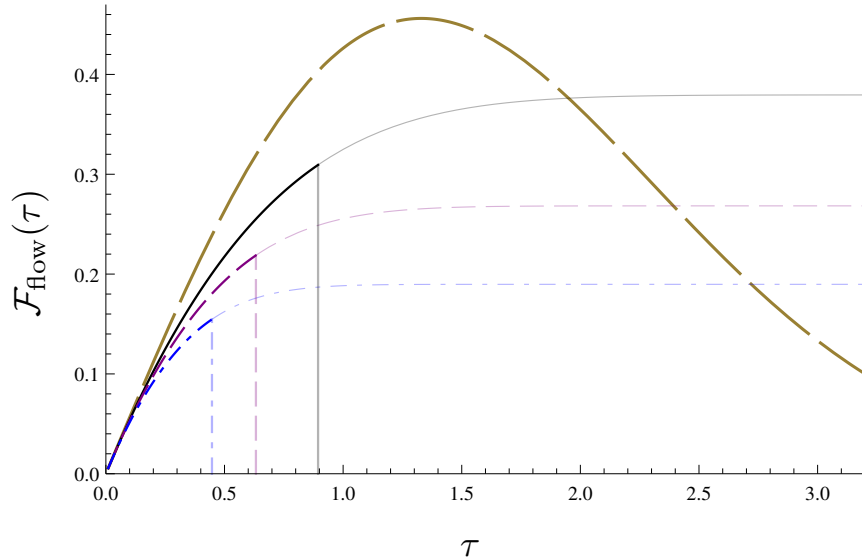


Figure 6. The rate of flow $\mathcal{F}_{\text{flow}}(\tau)$ as a function of τ for various physical regimes. The brown, long-dashed curve represents the function in Eq. (3.19), which corresponds to $x_c > 1$ and englobes both the ‘low energy’ regime, and the ‘intermediate energy’ one, depending upon the value of the upper limit $\tau_L = \sqrt{2x_c}$ on τ . The other curves correspond to different values $x_c < 1$ (i.e. to various ‘high-energy’ regimes) and are obtained according to Eq. (4.27): $x_c = 0.4$ (black, solid), $x_c = 0.2$ (purple, dashed), and $x_c = 0.1$ (blue, dashed-dotted). The thick lines represent the respective curves within their physical range of validity ($\tau < \tau_L$), whereas the thin curves are their extrapolations at larger times $\tau > \tau_L$. The vertical lines denote the upper time limit $\tau_L = \sqrt{2x_c}$.

As explained in Sect. 3, this is the rate at which the energy leaks out of the spectrum and accumulates into a condensate at $x = 0$. It is straightforward to numerically compute the integral in Eq. (4.27) and thus study the flow as a function of τ for various values $x_c \ll 1$. The results are shown in Fig. 6, together with the respective prediction of the ‘low-energy’ case $x_c > 1$, that is, the function $\mathcal{F}_{\text{flow}}(\tau)$ in Eq. (3.19). In principle, one should consider these curves only for τ values within the physically allowed range, i.e. for $\tau \leq \tau_L = \sqrt{2x_c}$. But in Fig. 6 we also show them for larger values $\tau > \tau_L$; this is interesting too, but for a different physical problem (see below).

By comparing curves which refer to different values of x_c , one can better appreciate the role of the kinematical constraint $x \leq x_c \ll 1$ in slowing down the branching process and thus reducing the energy flow. The plots in Fig. 6 make clear that, when lowering x_c , one reduces not only the total duration τ_L of the branching process, but also the rate for energy loss at any given time $\tau < \tau_L$. This trend is natural on physical grounds: by decreasing x_c , one limits the phase-space for medium-induced radiation to emissions which carry lower and lower fractions of the total energy of the leading particle. Fig. 6 also shows that the deviation between curves corresponding to different values of x_c increases with time; for $\tau \sim \tau_L$, this deviation is seen to be sizable including for the smallest values of x_c under consideration.

It would be interesting to understand the systematics of these plots via analytic studies. To that aim, one may attempt a small- τ expansion of the flow in Eq. (4.27) based on the corresponding

expansion of $\delta D_{\text{br}}(x, \tau)$ in Eq. (4.20). (This is tantamount to performing the small- ζ expansion of the function $\gamma(1/2, \zeta)$ in Eq. (4.27).) At leading order, one should use the dominant contribution to $\delta D_{\text{br}}(x, \tau)$, that is, (minus) the function $D_{\text{rad}}^{(1)}(x, \tau)$ in Eq. (4.22). One thus finds

$$\mathcal{F}_{\text{flow}}(\tau) \simeq - \int_0^{x_c} dx \frac{\partial}{\partial \tau} D_{\text{rad}}^{(1)}(x, \tau) = 2\bar{\alpha}^2 \tau \int_0^{x_c} \frac{dx}{\sqrt{x(x_c - x)}} = 2\pi\bar{\alpha}^2 \tau. \quad (4.28)$$

This estimate, which is independent of x_c , holds only for sufficiently small times, such that $\zeta(x_c, \tau) = \pi\bar{\alpha}^2\tau^2/x_c \ll 1$, where it describes indeed the common behavior of all the curves exhibited in Fig. 8. But this approximation is unable to capture the lift in degeneracy with increasing τ . One may expect to be able to compute corrections to Eq. (4.28) by using the higher order terms in the expansion (4.20) of D_{rad} , but this turns out not to be possible: for all the terms in this expansion beyond $D_{\text{rad}}^{(1)}$, the integral over x in Eq. (4.27) develops a non-integrable singularity at its upper endpoint x_c .

In the next subsection, we shall exploit the second equality in Eq. (4.25) to deduce an exact, analytic, result for $\mathcal{F}_{\text{flow}}(\tau)$ (see Eq. (4.39)). But for the purposes of the present discussion, it suffices to consider just one more term in the small- τ expansion of $\mathcal{F}_{\text{flow}}(\tau)$. This can be obtained by expanding the exact result in Eq. (4.39) and reads

$$\mathcal{F}_{\text{flow}}(\tau) \simeq 2\pi\bar{\alpha}^2 \tau \left(1 - \frac{\bar{\alpha}\tau}{\sqrt{x_c}} \right). \quad (4.29)$$

As expected, the corrective term above lifts the degeneracy between different values of x_c . The relative importance of this term increases with time and becomes independent of x_c when $\tau \sim \tau_L$ (since τ_L itself scales like $\sqrt{x_c}$): $\bar{\alpha}\tau_L/\sqrt{x_c} = \sqrt{2}\bar{\alpha}$. Hence, this correction would be negligible in the formal weak coupling limit, but it is numerically important for realistic values of $\bar{\alpha}$: e.g. $\sqrt{2}\bar{\alpha} \simeq 0.4$ for $\bar{\alpha} = 0.3$. And indeed, the inclusion of this correction greatly improves the accuracy of the small-time expansion, as it will be shown later, in Fig. 8: the limited expansion in Eq. (4.29) provides an excellent approximation to the exact result for any $\tau \leq \tau_L$.

Consider now the behavior of the flow for relatively large times $\tau \gg \tau_L$, that is, outside of the physical range for jet evolution. This corresponds to a different physical problem, which is closer to the familiar turbulence set-up — a steady source acts for arbitrarily large time and eventually builds up a time-independent energy spectrum —, except that our source has a rather unusual spectrum: rather than being localized near x_c (e.g. $\mathcal{S}(x) = \delta(x - x_c)$), the function $\mathcal{S}_0(x) = \bar{\alpha}/\sqrt{x}$ has a long tail at small $x \leq x_c$, as expected for *radiation*. The associated steady flow at large times can be obtained as follows: from Sect. 4.2 we recall that, when $\pi\bar{\alpha}^2\tau^2/x_c \gg 1$, the spectrum reaches the steady shape in Eq. (4.21) (see also Fig. 5). From that moment on, the energy contained in the spectrum cannot increase anymore. For this to be possible, the energy flux associated with branchings must precisely equilibrate the rate for energy injection by the source; that is, the r.h.s. of Eq. (4.24) must vanish:

$$\mathcal{F}(x_0, \tau) \simeq \int_{x_0}^{x_c} dx \mathcal{S}_0(x) = 2\bar{\alpha}(\sqrt{x_c} - \sqrt{x_0}). \quad (4.30)$$

As expected, this result is independent of time and fixed by the source. For $x_0 = 0$, it yields

$$\mathcal{F}_{\text{flow}}(\tau) \simeq 2\bar{\alpha}\sqrt{x_c} \quad \text{when} \quad \pi\bar{\alpha}^2\tau^2/x_c \gg 1, \quad (4.31)$$

which is indeed consistent with both the numerical results in Fig. 8 and the large-time asymptotics of Eq. (4.27), as one can easily check⁶.

⁶At large times, one has $\zeta \gg 1$ for any x , hence one can approximate $\gamma(1/2, \zeta) \simeq \sqrt{\pi}$ within Eq. (4.27).

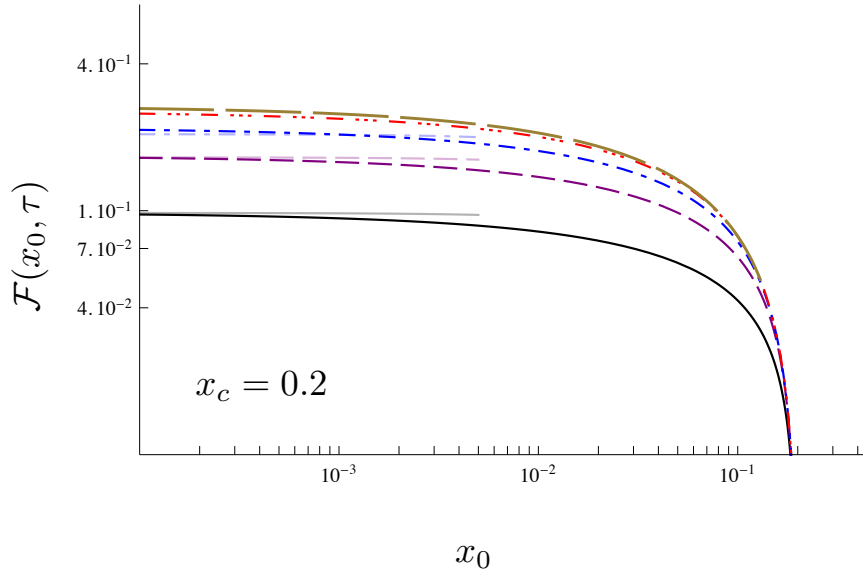


Figure 7. Plot (in log-log scale) of the energy flux $\mathcal{F}(x_0, \tau)$, cf. Eq. (4.26), as a function of x_0 for $\bar{\alpha} = 0.3$, $x_c = 0.2$, and various values of τ : $\tau = 0.2$ (solid, black), $\tau = 0.4$ (purple, dashed), $\tau = 0.63$ (blue, dashed-dotted), $\tau = 1$ (red, dashed-triple-dotted). The thin curves, shown for $\tau \leq \tau_L = 0.63$ and $x_0 \leq 0.005$, represent the approximation (4.34) valid at small τ and small x_0 . The enveloping curve (brown, long-dashed) is the limiting curve at large τ , cf. Eq. (4.30).

For comparison, let us also notice the spectrum and flux that would be generated by a localized source $\mathcal{S}(x) = A\delta(x-x_c)$ which acts for $\tau \geq 0$. (This problem has been already considered in Ref. [16].) For generic τ , the corresponding spectrum coincides (up to a factor of A) with the r.h.s. of Eq. (4.11) evaluated at $x_1 = x_c$. For large times $\pi\bar{\alpha}^2\tau^2/x_c \gg 1$, this reaches the steady shape

$$D_{\text{as}}(x) = \frac{A}{2\pi\bar{\alpha}} \sqrt{\frac{x_c}{x(x_c-x)}}. \quad (4.32)$$

In the same limit, the energy flux is both steady and strictly uniform, $\mathcal{F}_{\text{as}}(x_0) = A$, as in standard turbulence. For $x \ll x_c$, these results are consistent with the Kolmogorov–Obukhov relation (3.21).

It is finally interesting to study the x_0 -dependence of the energy flux in this high-energy case. This is expressed by Eq. (4.26) that we have plotted in Fig. 7 as a function of x_0 for different values of τ and for $x_c = 0.2$. Good analytic approximations can also be obtained. For relatively small times $\pi\bar{\alpha}^2\tau^2/x_c \ll 1$, and for x_0 not too close to x_c , it is convenient to rewrite Eq. (4.26) as

$$\mathcal{F}(x_0, \tau) = \mathcal{F}_{\text{flow}}(\tau) - \frac{\bar{\alpha}}{\sqrt{\pi}} \int_0^{x_0} \frac{dx}{\sqrt{x}} \gamma\left(\frac{1}{2}, \zeta\right). \quad (4.33)$$

When $\zeta \ll 1$, we can use the Taylor expansion of the function $\gamma(1/2, \zeta)$, which is rapidly converging. To the same accuracy as in Eq. (4.29), i.e. to second order in $\bar{\alpha}\tau$, it is enough to use $\gamma(1/2, \zeta) \simeq 2\sqrt{\zeta}$, which yields

$$\mathcal{F}(x_0, \tau) \simeq 2\pi\bar{\alpha}^2\tau \left\{ 1 - \frac{\bar{\alpha}\tau}{\sqrt{x_c}} - \frac{2}{\pi} \arcsin \sqrt{\frac{x_0}{x_c}} \right\}. \quad (4.34)$$

At larger times $\pi\bar{\alpha}^2\tau^2/x_c \gg 1$, and also for x_0 very close to x_c and any τ , the flux takes the form in Eq. (4.30). Both the numerical results in Fig. 7 and the analytic approximations in Eqs. (4.34) and (4.30) demonstrate that the flux associated with branchings is quasi-uniform (i.e. independent of x_0) for any $x_0 \ll x_c$. As already mentioned, this signals a phenomenon of wave turbulence. Additional evidence in that sense will emerge from the analysis in the next subsection.

4.4 The energy flux revisited: democratic branchings

In this subsection, we shall present an alternative calculation of the energy flux, which exploits the second equality in Eq. (4.25), i.e. the x -integral of the branching term $\mathcal{I}[D_{\text{rad}}]$. As we shall see, the main virtue of this alternative method is that it involves the gluon spectrum *quasi-locally in x* : in order to compute the flux $\mathcal{F}(x_0, \tau)$ at small $x_0 \ll x_c$, we need the spectrum $D_{\text{rad}}(x, \tau)$ at small $x \ll x_c$ as well. This property has important consequences, of both practical and conceptual nature. In practice, it will allow us to derive an exact analytic expression for the rate of flow $\mathcal{F}_{\text{flow}}(\tau) = \mathcal{F}(x_0 = 0, \tau)$ and to establish the analog of the Kolmogorov–Obhukov relation for the problem at hand. At a conceptual level, the locality of the branching process in energy (or in x) is a fundamental property of a turbulent process [29, 30]. This property is quite unusual in the context of a gauge theory, where splittings are generally very asymmetric due to the ‘infrared’ ($x \rightarrow 0$) singularity of bremsstrahlung. Its emergence in the context of the medium-induced gluon cascade [16, 22, 31] is a non-trivial consequence of coherence phenomena associated with multiple scattering, which lead to a profound modification in the splitting rate as compared to bremsstrahlung in the vacuum.

The integral of the branching term occurring in Eq. (4.25) can be decomposed as

$$-\int_{x_0}^{x_c} dx \mathcal{I}[D_{\text{rad}}](x, \tau) = \int_{x_0}^{x_c} dx \mathcal{L}(x, \tau) + \int_{x_0}^{x_c} dx \mathcal{G}(x, \tau), \quad (4.35)$$

where the two terms in the r.h.s. are the respective contributions of the ‘loss’ and ‘gain’ term in the rate equation. The ‘loss’ contribution is easily evaluated as

$$\int_{x_0}^{x_c} dx \mathcal{L}(x, \tau) = \int_0^1 dz z \mathcal{K}(z) \int_{x_0}^{x_c} dx \frac{D_{\text{rad}}(x, \tau)}{\sqrt{x}}. \quad (4.36)$$

In the ‘gain’ contribution, it is useful to change the integration variable as $x \rightarrow x' \equiv x/z$:

$$\begin{aligned} \int_{x_0}^{x_c} dx \mathcal{G}(x, \tau) &= - \int_{x_0}^{x_c} dx \int dz \Theta\left(z - \frac{x}{x_c}\right) \mathcal{K}(z) \sqrt{\frac{z}{x}} D_{\text{rad}}\left(\frac{x}{z}, \tau\right) \\ &= - \int dz z \mathcal{K}(z) \Theta\left(z - \frac{x_0}{x_c}\right) \int_{x_0/z}^{x_c} dx' \frac{D_{\text{rad}}(x', \tau)}{\sqrt{x'}}, \end{aligned} \quad (4.37)$$

where, in the second line, the upper limit x_c on x' follows from the condition $z > x/x_c$; also, the last Θ -function, which enforces $z > x_0/x_c$, guarantees that the lower limit x_0/z in the integral over x' remains smaller than the upper limit x_c . As usual, the ‘gain’ and ‘loss’ contributions taken separately develop singularities from the endpoint at $z = 1$ of the integral over z , but these singularities cancel in the sum of the two contributions. Hence, the overall result is well defined and reads

$$\mathcal{F}(x_0, \tau) = \bar{\alpha} \int_{x_0/x_c}^1 dz z \mathcal{K}(z) \int_{x_0}^{x_0/z} dx \frac{D_{\text{rad}}(x, \tau)}{\sqrt{x}} + \bar{\alpha} \int_0^{x_0/x_c} dz z \mathcal{K}(z) \int_{x_0}^{x_c} dx \frac{D_{\text{rad}}(x, \tau)}{\sqrt{x}}. \quad (4.38)$$

To better appreciate the physical interpretation of this result, let us return to the individual, ‘loss’ and ‘gain’, contributions, as shown in Eq. (4.36) and respectively Eq. (4.37).

The interpretation of the ‘loss’ term in Eq. (4.36) is quite clear: this is the energy transferred per unit time from one parton generation to the next one via the branching of any of the ‘hard’ modes with $x_0 < x < x_c$. (Recall that $\mathcal{K}(z)/\sqrt{x}$ represents the splitting rate for the parent mode x into daughter modes zx and $(1-z)x$. Also the factor of z within the first integral can be equivalently replaced by $z \rightarrow [z + (1-z)]/2 = 1/2$, due to the symmetry property $\mathcal{K}(z) = \mathcal{K}(1-z)$; hence, this factor truly accounts for the contribution of *both* daughter gluons.) However, some of these splittings do not contribute to the energy flux at x_0 : this is the case for the splittings with $zx > x_0$ (a condition which can be satisfied only for z values which are large enough, namely $z > x_0/x_c$), for which the daughter gluons are still harder than x_0 . The contributions of these splittings is therefore subtracted by the ‘gain’ term in Eq. (4.37), which is negative indeed. Accordingly, the net result is the sum of two types of contributions, represented by the two terms in the r.h.s. of Eq. (4.38): (i) relatively hard splittings with $x_0/x_c < z < 1$, but such the parent gluon x was close enough to x_0 (within the strip at $x_0 < x < x_0/z$), and (ii) relatively soft splittings with $z < x_0/x_c$, in which case the parent gluon can be located anywhere between x_0 and x_c .

The following observations are useful for what follows. In the limit where $x_0 \ll x_c$, the first term in the r.h.s of Eq. (4.38) dominates over the second one and controls the rate of flow. This is clear from the fact that the second term in Eq. (4.38) vanishes when $x_0 \rightarrow 0$, while the first one preserves a finite value in that limit, as we shall shortly see. Furthermore, still for $x_0 \ll x_c$, the second term is controlled by very asymmetric splittings ($z < x_0/x_c \ll 1$), whereas the first one is rather dominated by *quasi-democratic branchings*, that is, by generic z values in the bulk, which are not specially close to either the lower limit $z = x_0/x_c \ll 1$, or the upper limit $z = 1$, of the z -integral. Indeed, this integral is rapidly convergent both at small z , because of the factor of z in the integrand, and at $z \rightarrow 1$, because the result of the integral over x linearly vanishes in that limit. As already mentioned, the prominence of ‘quasi-democratic branchings’ is an essential condition for the emergence of wave turbulence: e.g. this permits the existence of fixed-point (KZ) solutions, which requires fine cancellations between the (*a priori* non-local) ‘gain’ term and the (always local) ‘loss’ term.

This locality allows us to construct an exact solution for the energy flux in the limit $x_0 \rightarrow 0$ and for the simplified kernel $\mathcal{K}_0(z)$ (for which the spectrum is analytically known). When $x_0 \rightarrow 0$, only the first term in Eq. (4.38) survives. The fact that the respective integral over z is not specially sensitive to its lower limit x_0/x_c means that the relevant values of z do *not* scale like x_0 when $x_0 \rightarrow 0$. Hence, the upper limit x_0/z of the integral over x vanishes when $x_0 \rightarrow 0$, so like the corresponding lower limit. Accordingly, this integral is controlled by very small values of x , which scale like x_0 and in particular are much smaller than x_c . It is then justified to evaluate this integral using the dominant behavior of the spectrum for $x \ll x_c$, that is, the KZ spectrum in Eq. (4.18). With this scaling behavior $\sim 1/\sqrt{x}$, the integral over x is logarithmic and its result is independent of x_0 . One thus finds

$$\mathcal{F}_{\text{flow}}(\tau) = 2\pi\bar{\alpha}^2\tau [1 - h(\zeta_0)], \quad \zeta_0 \equiv \zeta(x_c, \tau) = \frac{\pi\bar{\alpha}^2\tau^2}{x_c}, \quad (4.39)$$

where the overall factor 2π has been generated as

$$2\pi = \int_0^1 dz z \mathcal{K}_0(z) \ln \frac{1}{z} = \int_0^1 dz \frac{1}{\sqrt{z}(1-z)^{3/2}} \ln \frac{1}{z}. \quad (4.40)$$

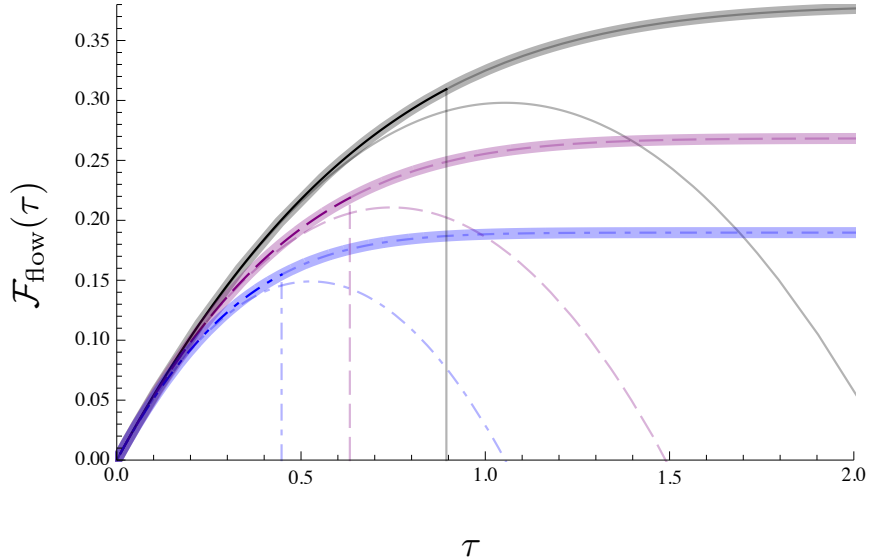


Figure 8. The rate of flow $\mathcal{F}_{\text{flow}}(\tau)$ as a function of τ in the high-energy regime for various values of x_c : $x_c = 0.4$ (black, solid), $x_c = 0.2$ (purple, dashed), and $x_c = 0.1$ (blue, dashed-dotted). The thick lines represent the respective curves within their physical range of validity ($\tau < \sqrt{2x_c}$), as computed by numerical integration in Eq. (4.26). The thin curves following the thick ones are the predictions of Eq. (4.26) for larger times, outside the physical range ($\tau > \sqrt{2x_c}$). The thin curves deviating from the thick ones correspond to the limited expansion in Eq. (4.29). Finally, the very thick (opaque) curves are the new, fully explicit, analytic result in Eq. (4.39). The vertical lines denote the physical upper limit on time $\tau_L = \sqrt{2x_c}$.

Using the properties of the function $h(\zeta)$ discussed in Sect. 4.2, one can easily check both the small- τ expansion of the flow, as anticipated in Eq. (4.29), and its large- τ asymptotics in Eq. (4.31). As a check of Eq. (4.39), we display this result in Fig. 8 (as a function of τ for several values of x_c) versus the result of the numerical integration in Eq. (4.26). One can also see in this figure that the limited expansion (4.29) is indeed a very good approximation for any τ in the physical range, as already noticed in Sect. 4.3. This is understandable since the first correction beyond Eq. (4.29) in the small- τ expansion of Eq. (4.39) is exactly vanishing, as manifest on Eq. (4.20).

By inspection of Eqs. (4.18) and (4.39), it is obvious that the spectrum at small x is proportional to the flow, in the sense of Eq. (3.21). The above construction of Eq. (4.39) explains the physical origin of this proportionality and also suggests that it is quite general: it holds for any splitting kernel with the singularity structure shown in Eq. (3.6), since any such a kernel leads to democratic branchings and to a spectrum which at small x has the shape of the scaling spectrum $D_{\text{sc}}(x) = 1/\sqrt{x}$. The time dependence of the spectrum (again at small x) depends upon the detailed structure of the branching kernel (it is generally different for the full kernel $\mathcal{K}(z)$ and for the simplified one $\mathcal{K}_0(z)$), and also upon the nature of the ‘source’ at large x (it is e.g. different for a source localized at x_c , $\mathcal{S}(x) = A\delta(x - x_c)$, as opposed to a radiation source $\mathcal{S}_0(x) = \theta(x_c - x)\bar{\alpha}/\sqrt{x}$). But the rate of flow $\mathcal{F}_{\text{flow}}(\tau)$ has exactly the same time-dependence as the spectrum, and the proportionality relation (3.21) universally holds,

with a proportionality factor which is kernel–dependent though:

$$D(x, \tau) \simeq \frac{1}{v\bar{\alpha}} \frac{\mathcal{F}_{\text{flow}}(\tau)}{\sqrt{x}} \quad \text{for } x \ll x_c. \quad (4.41)$$

Here, v is a pure number, defined by the obvious generalization of Eq. (4.40) :

$$v \equiv \int_0^1 dz z \mathcal{K}(z) \ln \frac{1}{z} = \int_0^1 dz \frac{f(z)}{\sqrt{z}(1-z)^{3/2}} \ln \frac{1}{z} \simeq 4.96. \quad (4.42)$$

On both Eq. (4.42) or Eq. (4.40), it is obvious that the respective integral over z is dominated by generic values in the bulk, as expected for quasi–democratic branchings. As discussed after Eq. (3.14), v has the physical interpretation of the average number of soft primary gluons with energies $\omega \sim \omega_s(t) = \bar{\alpha}^2 \hat{q} t^2 / 2$ that are emitted by the leading particle during a time t .

Eq. (4.41) is particularly useful in a steady situation, where the energy flux is *a priori* known, since determined by the external source. (This is the case in the familiar turbulence problem, where the Kolmogorov–Obhukov relation has been originally identified.) As a simple, yet non–trivial, application of this type, consider the steady situation reached when the external source $\mathcal{S}_0(x) = \theta(x_c - x)\bar{\alpha}/\sqrt{x}$ acts for sufficiently large time $\bar{\alpha}^2 \tau^2 \gg x_c$. The corresponding flow is given by Eq. (4.31) and then Eq. (4.41) can be used to deduce the asymptotic spectrum at large times and small x :

$$D(x, \tau \rightarrow \infty) \simeq \frac{2}{v} \sqrt{\frac{x_c}{x}} \quad \text{for } x \ll x_c. \quad (4.43)$$

This result is interesting in that it represents a non–perturbative prediction associated with the full kernel, for which exact analytic solutions are not known. (For the simplified kernel, $v \rightarrow 2\pi$ and Eq. (4.43) reduces to Eq. (4.21), as it should.)

Still for the full kernel, Eq. (4.41) can also be used in the reversed way, namely to deduce the flow from the spectrum in the small–time regime at $\bar{\alpha}^2 \tau^2 \ll x_c$. Indeed, in this limit and for $x \ll x_c$, the spectrum can be computed in perturbation theory, via iterations (see the discussion in Appendix A). To second order in $\bar{\alpha}\tau$, the result turns out to be the same as for the simplified kernel $\mathcal{K}_0(z)$, namely (compare to Eq. (4.20))

$$D_{\text{rad}}(x, \tau) \simeq \frac{\bar{\alpha}\tau}{\sqrt{x}} \left(1 - \frac{\bar{\alpha}\tau}{\sqrt{x_c}} \right) \quad \text{for } \bar{\alpha}^2 \tau^2 \ll x_c \quad \text{and} \quad x \ll x_c. \quad (4.44)$$

By using this approximation together with Eq. (4.41), we can obtain the generalization of Eq. (4.29) to the case of the complete kernel:

$$\mathcal{F}_{\text{flow}}(\tau) = v\bar{\alpha}^2 \tau \left(1 - \frac{\bar{\alpha}\tau}{\sqrt{x_c}} \right). \quad (4.45)$$

This result is quite useful, in particular for phenomenology, in that it offers a rather accurate estimate for the energy loss via flow for the case of the physical kernel. This will be further discussed in the next section. In Fig. 9 we show the numerical solution to the rate equation (4.8) with the full splitting kernel \mathcal{K} in Eq. (3.6), together with its analytic approximations valid at small x : Eq. (4.44) at small τ and Eq. (4.43) at large τ . In particular, we have checked that this special number $v \simeq 4.96$ can be indeed read off the asymptotic behavior of the numerical solution at large time, in agreement with Eq. (4.43).

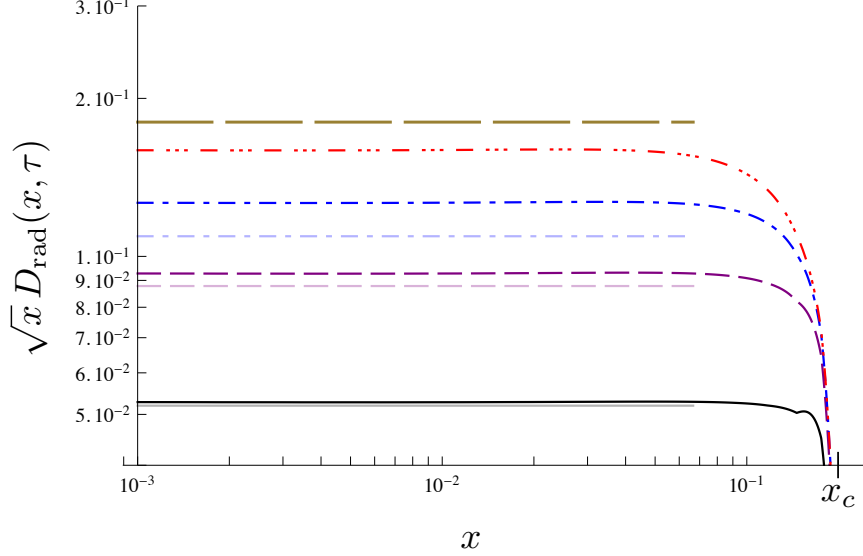


Figure 9. The numerical solution to the rate equation Eq. (4.8) with the full splitting kernel \mathcal{K} from Eq. (3.6), for $x_c = 0.2$ and various values of τ : $\tau = 0.2$ (solid, black), $\tau = 0.4$ (purple, dashed), $\tau = 0.63$ (blue, dashed–dotted), $\tau = 1$ (red, dashed–triple–dotted). The thin curves, shown for $\tau \leq \tau_L = 0.63$ and $x \leq 0.07$, represent the small- τ and small- x approximation in Eq. (4.44). The enveloping curve (brown, long-dashed) is the limiting curve at large τ , cf. Eq. (4.43).

5 Physical discussion: energy loss at large angles

In this section, we shall summarize the results obtained in the previous sections and use them to compute one of the most interesting observables for the phenomenology of di-jet asymmetry at the LHC: the energy lost by the gluon cascade via soft quanta propagating at large angles. Specifically, we shall successively consider the following quantities:

(i) *the flow energy* $\mathcal{E}_{\text{flow}}(\tau)$: this is the energy fraction carried away by the turbulent flow and which formally ends up in a condensate at $x = 0$;

(ii) *the thermalization energy* $\mathcal{E}_{\text{th}}(\tau)$: this is the energy fraction which is carried by quanta with $x < x_{\text{th}} \equiv T/E$, which are assumed to thermalize and hence transmit their energy to the medium. (As in Sect. 3, we assume that the thermalization mechanism acts as a ‘perfect sink’, i.e. it does not modify the energy flux at $x \geq x_{\text{th}}$; cf. the discussion at the end of Sect. 3.3.)

(iii) *the energy transported at angles larger than a given value* θ_0 : the definition of this quantity requires some additional discussion and is postponed after the study of the two previous ones.

The *flow energy* can be calculated in two alternative ways: as the τ -integral of the respective flux $\mathcal{F}_{\text{flow}}(\tau)$, which is explicitly given by Eq. (4.39), or as the x -integral of the change $\delta D_{\text{br}}(x, \tau)$ in the spectrum due to branchings, as shown in Eq. (4.15):

$$\mathcal{E}_{\text{flow}}(\tau) \equiv \int_0^\tau d\tau' \mathcal{F}_{\text{flow}}(\tau') = \int_0^{x_c} dx \delta D_{\text{br}}(x, \tau). \quad (5.1)$$

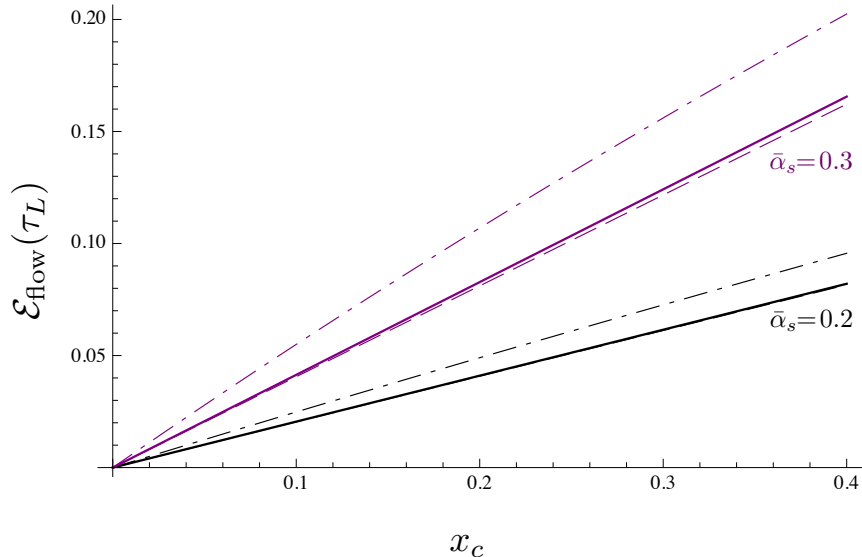


Figure 10. The energy fraction $\mathcal{E}_{\text{flow}}(\tau_L)$ carried by the turbulent flow, i.e. Eq. (5.1) with $\tau = \tau_L \equiv \sqrt{2x_c}$, plotted as a function of x_c for two values of the coupling constant: $\bar{\alpha} = 0.2$ (black) and $\bar{\alpha} = 0.3$ (purple). Solid lines: the exact result obtained by numerical integration in the second equality in Eq. (5.1). Dashed lines: the weak-coupling expansion in Eq. (5.2), that is, $\mathcal{E}_{\text{flow}} = 2\pi\bar{\alpha}^2 x_c (1 - 2\sqrt{2}\bar{\alpha}/3)$. (For $\bar{\alpha} = 0.2$, this approximation can hardly be distinguished from the exact curve.) For comparison, we also show, with dashed-dotted lines, the respective predictions of the ‘low-energy case’, i.e. Eq. (3.13) with $\tau = \sqrt{2x_c}$.

The second representation above relies on the fact that the flow energy is by definition the difference between the total energy supplied by the source $\mathcal{S}_0(x)$ and the radiation energy which remains in the spectrum. Here, we shall use this second representation to numerically compute $\mathcal{E}_{\text{flow}}$, but rely on the first one for analytic estimates. Indeed, we know that already the limited expansion of the flow shown in Eq. (4.45) is very accurate for any $\tau \leq \tau_L$; this can be easily integrated over time to give

$$\mathcal{E}_{\text{flow}}(\tau) \simeq \frac{v}{2} \bar{\alpha}^2 \tau^2 \left(1 - \frac{2}{3} \frac{\bar{\alpha}\tau}{\sqrt{x_c}} \right). \quad (5.2)$$

This estimate holds for the full kernel $\mathcal{K}(z)$, but the corresponding result for the simplified kernel $\mathcal{K}_0(z)$ is simply obtained by replacing $v \rightarrow 2\pi$ in the prefactor.

In Fig. 10 we show the flow energy evaluated at the end of the evolution ($\tau = \tau_L = \sqrt{2x_c}$) as a function of x_c and for two values of $\bar{\alpha}$. We here compare the respective exact results, cf. Eq. (5.1), with the limited expansion in Eq. (5.2) (which is seen to be quite accurate) and with the prediction (3.13) of the ‘low-energy case’ which here is extrapolated to $x_c \ll 1$, that is, outside its physical range of validity. The purpose of this extrapolation is to emphasize that, by ignoring the kinematical constraint $x \leq x_c$, one would significantly overestimate the energy loss via flow. Remarkably, the plots in Fig. 10 show that the quantity $\mathcal{E}_{\text{flow}}(\tau_L)$ is a linear function of x_c . This property is obvious for the limited expansion in Eq. (5.2), but is in fact exact within the present effective theory, as we now show.

Namely, by using Eq. (4.15) for $\delta D_{\text{br}}(x, \tau)$, we can write

$$\mathcal{E}_{\text{flow}}(\tau_L) = \bar{\alpha}\tau_L \int_0^{x_c} \frac{dx}{\sqrt{x}} h\left(\frac{\pi\bar{\alpha}^2\tau_L^2}{x_c - x}\right) = \sqrt{2}\bar{\alpha}x_c \int_0^1 \frac{du}{\sqrt{u}} h\left(\frac{2\pi\bar{\alpha}^2}{1-u}\right), \quad (5.3)$$

where the r.h.s. is indeed linear in x_c , as anticipated. This is interesting in that it implies that the energy which is lost via flow, namely (cf. Eq. (5.2)),

$$\Delta E_{\text{flow}} \equiv E \mathcal{E}_{\text{flow}}(\tau_L) \simeq v \bar{\alpha}^2 \omega_c \left(1 - \frac{2\sqrt{2}}{3}\bar{\alpha}\right), \quad (5.4)$$

is independent of the energy E of the leading particle and parametrically of order $\bar{\alpha}^2 \omega_c = \omega_s^2$ (the natural energy scale for multiple branchings). One should however keep in mind that this conclusion holds only for sufficiently energetic jets, such that $x_c \ll 1$, or $E \gg \omega_c$. Notice also that the actual value of the energy loss in Eq. (5.4) is enhanced by the relatively large numerical factor $v(1 - 2\sqrt{2}\bar{\alpha}/3)$ ($\simeq 3.5$ for $\bar{\alpha} = 0.3$) as compared to its parametric estimate $\bar{\alpha}^2 \omega_c$. This is mostly due to the factor $v \simeq 4.96$, which we recall is the average number of soft primary emissions with energies $\omega \sim \omega_s$.

Given the flow energy in Eq. (5.1), the *thermalization energy* can immediately be computed as the sum between $\mathcal{E}_{\text{flow}}(\tau)$ and the energy contained in the small- x bins of the spectrum:

$$\mathcal{E}_{\text{th}}(\tau) = \mathcal{E}_{\text{flow}}(\tau) + \int_0^{x_{\text{th}}} dx D_{\text{rad}}(x, \tau). \quad (5.5)$$

In practice, $x_{\text{th}} \ll x_c$, hence the above integral can be estimated by using the dominant behavior of the spectrum for $x \ll x_c$. To the same accuracy as in Eq. (5.2), one finds

$$\mathcal{E}_{\text{th}}(\tau) \simeq \frac{v}{2} \bar{\alpha}^2 \tau^2 \left(1 - \frac{2}{3} \frac{\bar{\alpha}\tau}{\sqrt{x_c}}\right) + 2\bar{\alpha}\tau \sqrt{x_{\text{th}}} \left(1 - \frac{\bar{\alpha}\tau}{\sqrt{x_c}}\right). \quad (5.6)$$

We emphasize that this result, which holds for the complete kernel (3.6), is fully obtainable from perturbation theory: it only requires the second iteration to the spectrum in Eq. (4.44). As manifest in Eq. (5.6), the flow contribution to $\mathcal{E}_{\text{th}}(\tau)$ is formally of higher order in $\bar{\alpha}\tau$, yet it dominates over the ‘spectrum’ contribution as soon as x_{th} is small enough: for $\tau = \tau_L$, the flow dominates provided $x_{\text{th}} < x_s = \bar{\alpha}^2 x_c$ (or, equivalently, $T < \omega_s$), a condition which is well satisfied in practice (see below).

In Fig. 11 we plot $\mathcal{E}_{\text{th}}(\tau_L)$ as a function of x_{th} for $x_c = 0.2$ and $x_c = 0.4$, and for the simplified kernel \mathcal{K}_0 . The exact result as obtained via numerical integration in Eq. (5.5) is compared to the limited expansion in Eq. (5.6) (where we replace $v \rightarrow 2\pi$, of course).

We now turn to the third quantity introduced above, namely the energy fraction which after a time τ has been transported at angles larger than a given value θ_0 . We denote this quantity as $\mathcal{E}(\theta > \theta_0, \tau)$. So far, we have considered only the energy distribution for the gluons in the cascade, but not also their distribution in transverse momentum \mathbf{k} , or in the polar angle θ w.r.t. the jet axis (defined as $\sin \theta = k_{\perp}/\omega$). Rather, the \mathbf{k} -distribution has been explicitly integrated out, as shown in Eq. (3.1), in order to obtain simpler versions for the rate equations. Yet, it turns out that for qualitative and even semi-quantitative estimates, one can restore the θ -distribution via the following, simple, argument. All the gluons in the cascade which are not too soft (namely, those with energy fractions $x \gtrsim x_s = \bar{\alpha}^2 x_c$) propagate in the medium along a distance of order L and hence accumulate via multiple scattering an average transverse momentum squared $\langle k_{\perp}^2 \rangle \simeq Q_L^2 \equiv \hat{q}L$, which is independent of x . So long as

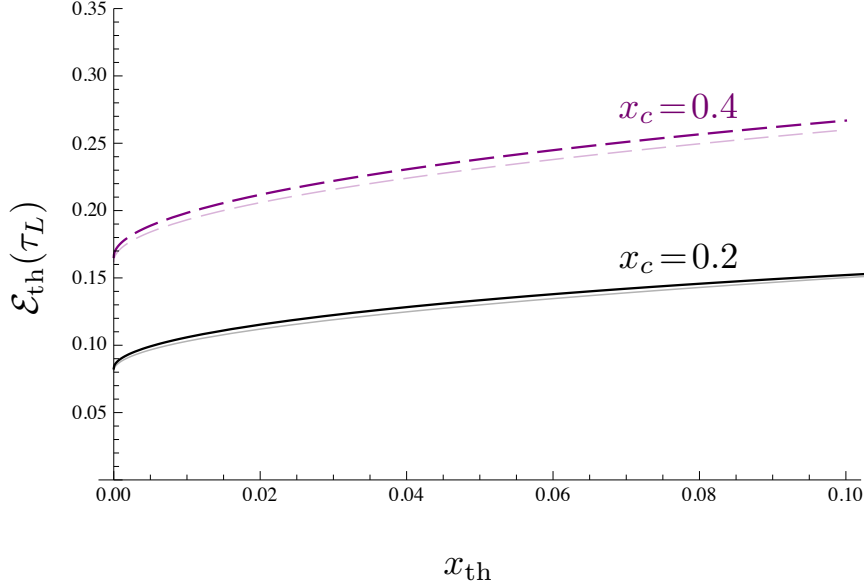


Figure 11. The energy fraction which ‘thermalizes’ $\mathcal{E}_{\text{th}}(\tau_L)$, plotted as a function of the thermalization scale x_{th} for two values of x_c : $x_c = 0.4$ (black, solid) and $x_c = 0.2$ (purple, dotted). The thick curves are the exact result obtained via numerical integration in Eq. (5.5). The thin, opaque, curves are the respective predictions of the limited expansion in Eq. (5.6) with $v \rightarrow 2\pi$.

this momentum Q_L is much smaller than the gluon energy $\omega = xE$, one can estimate the propagation angle according to

$$\theta(x) \simeq \frac{Q_L}{xE} = \frac{x_c}{x} \theta_c, \quad \text{with} \quad \theta_c \equiv \frac{Q_L}{\omega_c} = \frac{2}{\sqrt{\hat{q}L^3}}. \quad (5.7)$$

Hence, the interesting quantity $\mathcal{E}(\theta > \theta_0, \tau)$ can be computed as the energy fraction $\mathcal{E}^<(x_0, \tau)$ carried by the gluons with $x < x_0$, where $x_0 \simeq x_c(\theta_c/\theta_0)$. This is of course the same as the ‘thermalization energy’ in Eq. (5.5) evaluated for $x_{\text{th}} = x_0$. Hence, plotting the following quantity

$$\mathcal{E}^<(x_0, \tau) \equiv \mathcal{E}_{\text{flow}}(\tau) + \int_0^{x_0} dx D_{\text{rad}}(x, \tau) \quad (5.8)$$

as a function of x_c/x_0 is tantamount to representing the quantity $\mathcal{E}(\theta > \theta_0, \tau)$ as a function of θ_0/θ_c . This is strictly true so long as the angle θ_0 is not too large, namely $\theta_0 \lesssim \theta_c/\bar{\alpha}^2$, in order for the condition $x_0 \gtrsim x_s$ to remain satisfied⁷. But as we argue now, this is not a serious limitation. Indeed, we have previously explained that, when $x_0 < x_s$, the r.h.s. of Eq. (5.8) is dominated by the first piece, the flow energy, which is independent of x_0 (recall the discussion after Eq. (5.6)). Hence, for θ_0 larger than $\theta_s \equiv \theta(x_s) \simeq \theta_c/\bar{\alpha}^2$, the function $\mathcal{E}(\theta > \theta_0, \tau)$ is quasi-independent of x_0 and approximately equal to $\mathcal{E}_{\text{flow}}(\tau)$. An intuitive view of the angles θ_c and θ_s in the context of a typical gluon cascade is provided by Fig. 1.

⁷ The softer gluons with $x \lesssim x_s$ have a shorter lifetime $\Delta t(x) < L$, as shown in Eq. (3.22). The corresponding transverse momentum broadening is estimated as $\langle k_{\perp}^2 \rangle(x) \sim \hat{q}\Delta t(x)$, and the relation (5.7) between the propagation angle $\theta(x)$ and the reference angle θ_c gets replaced by (to parametric accuracy) $\theta(x)/\theta_c \sim (1/\sqrt{\bar{\alpha}})(x_c/x)^{3/4}$ [18–20].

As a side remark, we observe that the total energy carried by gluons with energies smaller than a given scale ω_0 , with $\omega_0 \leq \omega_c$, which is computed as (below, $x_0 \equiv \omega_0/E \leq x_c$)

$$\Delta E^<(\omega_0) = E \mathcal{E}^<(x_0, \tau_L), \quad (5.9)$$

is independent of the energy E of the LP (within the present approximations), but only depends upon the medium scale ω_c and upon the energy scale ω_0 of reference. This follows via manipulations in Eq. (5.8) which are entirely similar to those in Eq. (5.3).

Returning to Eq. (5.8), we notice that, in practice, it is more convenient to plot the complementary quantity, namely the energy fraction located at x -values *larger* than x_0 ,

$$\begin{aligned} \mathcal{E}^>(x_0, \tau) &\equiv 1 - \mathcal{E}^<(x_0, \tau) = \mathcal{E}_{\text{LP}}(\tau) + \mathcal{E}(x_0, x_c, \tau) \\ &= 1 - 2\bar{\alpha}\tau\sqrt{x_c} + \int_{x_0}^{x_c} dx D_{\text{rad}}(x, \tau) \\ &= 1 - 2\bar{\alpha}\tau\sqrt{x_0} - \int_{x_0}^{x_c} dx \delta D_{\text{br}}(x, \tau). \end{aligned} \quad (5.10)$$

Indeed, this corresponds better to the quantity which is actually measured in the experiments: the jet energy $E_J(\theta_0)$ as a function of the jet opening angle θ_0 (i.e. the total energy in the gluon cascade which propagates along angles $\theta \leq \theta_0$). As emphasized in the second equality above, this quantity $\mathcal{E}^>(x_0, \tau)$ is the sum of the energy fractions carried by the leading particle and by the modes at $x_0 < x < x_c$.

In Fig. 12, the quantity in Eq. (5.10) is represented as a function of x_c/x_0 for $\tau = \tau_L$ and $x_c = 0.4$. One also shows there the single-branching (or BDMPSZ) approximation, $\mathcal{E}^>(x_0, \tau_L) = 1 - 2\bar{\alpha}\sqrt{2x_c x_0}$, which is obtained by neglecting the integral of δD_{br} in the third line of Eq. (5.10), as well as the respective prediction of the low-energy case, Eq. (3.16), which here is extrapolated outside its physical range. Two features of these curves are worth emphasizing:

First, the ‘offset’ at large x_c/x_0 , i.e. the fact that, for the two curves which include the effects of multiple branchings, the difference $1 - \mathcal{E}^>(x_0) = \mathcal{E}^<(x_0)$ approaches a finite value as $x_c/x_0 \rightarrow \infty$. This non-zero value is, of course, the energy fraction $\mathcal{E}_{\text{flow}}$ taken away by the turbulent flow. As also visible in Fig. 12 (and obvious on physical grounds), this offset is absent if one neglects multiple branchings, i.e. if one tries to describe the energy distribution at large angles on the basis of the BDMPSZ spectrum alone. For applications to the phenomenology, it is important to notice that the kinematic restriction to $x < x_c$ (which applies whenever $x_c < 1$) significantly reduces the value of this offset. This reduction is visible in both Fig. 12 and Fig. 10.

Second, as also visible in Fig. 12 (and anticipated after Eq. (5.8)), the variation with x_c/x_0 is extremely slow, especially for the two curves which include the effects of multiple branchings. Physically, this means that, by increasing the jet opening angle $\theta_0 = (x_c/x_0)\theta_c$, one can recover some of the energy that has been transported at large angles, *but only very slowly*. This is so because most of this energy has been transported, by the turbulent flow, directly at very large angles $\theta \gtrsim \theta_{\text{th}}$, where it has been lost towards the medium via thermalization. Here, θ_{th} is the propagation angle for the very soft quanta with $x \sim x_{\text{th}}$ and is significantly larger than θ_s (since x_{th} is much smaller than $x_s = \bar{\alpha}^2 x_c$). In principle, this angle θ_{th} can be estimated within our effective theory — to parametric accuracy one finds $\theta_{\text{th}}/\theta_c \sim (1/\sqrt{\bar{\alpha}})(x_c/x_{\text{th}})^{3/4}$, cf. footnote 7 —, but this estimate is probably questionable: the angular distribution of the very soft gluons with $x \sim x_{\text{th}}$ could be influenced by other effects, like the precise mechanism of thermalization, the Bethe–Heitler limit on the medium-induced radiation, or the

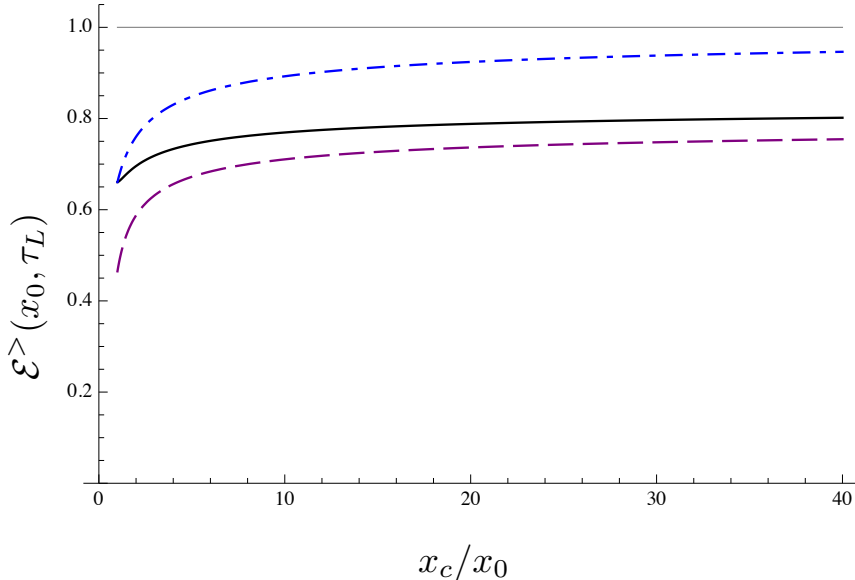


Figure 12. The energy $\mathcal{E}^>(x_0, \tau_L)$ contained in the bins of the spectrum with $x \geq x_0$ at the end of the evolution plotted as a function of x_c/x_0 for $x_0 \leq x_c$, $x_c = 0.4$, and $\bar{\alpha} = 0.3$. Black, solid, curve: the full result computed according to Eq. (5.10). Blue, dotted-dashed, curve: the approximation obtained by neglecting the effects of multiple branchings. Purple, dashed, curve: the respective prediction of the low-energy case, Eq. (3.16), which is extrapolated to $x_c = 0.4$. As explained in the text, these curves can also be viewed as representing the energy fraction $\mathcal{E}_J(\theta_0)$ contained within a jet with opening angle θ_0 plotted as a function of θ_0/θ_c .

kinematic constraint $k_\perp < \omega$, which are not properly included in the current formalism. Fortunately though, this theoretical uncertainty is not important for the angular distribution of the energy loss: the relevant curves in Fig. 12 are essentially flat for $x_c/x_0 \gtrsim 1/\bar{\alpha}^2 \simeq 10$, i.e. for angles $\theta_0 \gtrsim \theta_s$.

Let us conclude with a few numerical estimates in view of the phenomenology. Recent theoretical analyses of the data support an average value for the jet quenching parameter in the ballpark of $\hat{q} = 1 \text{ GeV}^2/\text{fm}$ [33]. By also choosing an average length $L = 4 \text{ fm}$ for the in-medium path, one finds $\omega_c \simeq 40 \text{ GeV}$ and $\theta_c \simeq 0.05$. This implies that the characteristic scale for multiple branching is quite hard, $\omega_s = \bar{\alpha}^2 \omega_c \simeq 4 \text{ GeV}$, and in particular significantly harder than the medium ‘temperature’ $T \lesssim 1 \text{ GeV}$ (the average transverse momentum of the medium constituents). In the measurements of di-jet asymmetry at the LHC, one has $E \geq 100 \text{ GeV}$; this energy is sufficiently large compared to ω_c for the ‘high-energy’ regime ($E \gg \omega_c$) to apply.

In this regime, the energy ΔE_{flow} lost by the gluon cascade via flow is independent of the original energy E (cf. the discussion after Eq. (5.4)). Using Eq. (5.4) with $\omega_c = 40 \text{ GeV}$ and $\bar{\alpha} = 0.3$, one finds

$$\Delta E_{\text{flow}} \simeq 0.32 \omega_c \simeq 13 \text{ GeV}. \quad (5.11)$$

It is also interesting to compute the energy transported at angles larger than $\theta_s = \theta_c/\bar{\alpha}^2 \simeq 0.5$. This is obtained from Eq. (5.9) with $\omega_0 \rightarrow \omega_s$ and, once again, is independent of the energy E of the LP. A good estimate is given by Eq. (5.6) with $x_{\text{th}} \rightarrow x_s = \bar{\alpha}^2 x_c$, and reads

$$\Delta E(\theta > \theta_s = 0.5) = E \mathcal{E}^<(x_s, \tau_L) \simeq \Delta E_{\text{flow}} + 2\sqrt{2}\bar{\alpha}^2 \omega_c (1 - \sqrt{2}\bar{\alpha}) \simeq 19 \text{ GeV}. \quad (5.12)$$

The above numbers compare reasonably well with the corresponding experimental results [2, 8], especially in view of our crude assumptions concerning the structure of the medium.

Consider finally the variation of the jet energy with increasing the jet opening angle θ_0 , i.e. the function $E_J(\theta_0)$. Our results in Fig. 12 predict that this quantity should be very slowly increasing with θ_0 . This seems to significantly differ from a recent analysis of the experimental data in Pb+Pb collisions at the LHC, which has reported a considerably steeper angular dependence for $E_J(\theta_0)$ [8]. Note however that a similarly steep dependence has also been found in the corresponding data for p+p collisions, and that the *difference* between these two sets of data looks essentially flat (as a function of θ_0) within the error bars [8]. It looks reasonable to interpret this difference as a measure of the medium effects in heavy ion collisions. If so, the fact that this difference appears to be slowly varying with θ_0 (in fact, almost flat) is in good agreement with our predictions in Fig. 12.

Acknowledgments

We are grateful to Al Mueller for insightful comments on the manuscript. We acknowledge useful related discussions with Jean-Paul Blaizot and Yacine Mehtar-Tani. This research is supported by the European Research Council under the Advanced Investigator Grant ERC-AD-267258. Figure 1 has been made with Jaxodraw [41].

A Perturbation theory for the rate equation

In this Appendix, we shall discuss the perturbative solution to the rate equation with a source, Eq. (4.8), as obtained via successive iterations of the branching term $\bar{\alpha}\mathcal{I}[D_{\text{rad}}]$ in the r.h.s. This is tantamount to an expansion in powers of $\bar{\alpha}\tau$ in which the source term $\mathcal{S}_0(x) = \bar{\alpha}/\sqrt{x}$ (including its factor $\bar{\alpha}$) is treated as a quantity of $\mathcal{O}(1)$. The zeroth order result is $D_{\text{rad}}^{(0)} = \bar{\alpha}\tau/\sqrt{x}$, while the first iteration, as obtained by evaluating the branching term $\bar{\alpha}\mathcal{I}[D_{\text{rad}}]$ with the zeroth order result and integrating over τ , yields

$$D_{\text{rad}}^{(1)}(x, \tau) = \frac{\bar{\alpha}^2\tau^2}{2} \int dz \mathcal{K}(z) \left\{ \Theta\left(z - \frac{x}{x_c}\right) \frac{z}{x} - \frac{z}{x} \right\} = -\frac{\bar{\alpha}^2\tau^2}{2x} \int_0^{x/x_c} dz z \mathcal{K}(z). \quad (\text{A.1})$$

The net result, which is negative, is due to an excess in the phase-space for the loss term, at $z < x/x_c$. To simplify the final integral over z , we shall restrict ourselves to the simplified kernel $\mathcal{K}_0(z)$. In that case, one can easily compute (say, by changing the integration variable as $z \equiv (u - 1)/u$)

$$\int_0^{x/x_c} dz z \mathcal{K}_0(z) = \int_0^{x/x_c} \frac{dz}{\sqrt{z}(1-z)^{3/2}} = 2\sqrt{\frac{x}{x_c - x}}. \quad (\text{A.2})$$

When inserted into Eq. (A.1), this confirms the result (4.22) for $D_{\text{rad}}^{(1)}$.

Note that the small- x limit (in the sense that $x/x_c \ll 1$) of the result in Eq. (A.2) would be the same for the full kernel $\mathcal{K}(z)$: indeed, when $z < x/x_c \ll 1$, one can approximate $f(z) \simeq 1$ in Eq. (3.6). This confirms that the limited expansion shown in Eq. (4.44) holds for the physical kernel.

Returning to the simplified kernel $\mathcal{K}_0(z)$, in which case Eq. (A.2) holds for any $x < x_c$, let us also compute the second iteration, by evaluating the branching term with the first order correction in

Eq. (4.22). One can write

$$\begin{aligned} \mathcal{I}[D_{\text{rad}}^{(1)}](x, \tau) &= -\frac{\bar{\alpha}^2 \tau^2}{x} \int dz z \mathcal{K}(z) \left\{ \Theta\left(z - \frac{x}{x_c}\right) \frac{1}{\sqrt{x_c - x/z}} - \frac{1}{\sqrt{x_c - x}} \right\} \\ &= \frac{2\bar{\alpha}^2 \tau^2}{\sqrt{x}(x_c - x)} - \frac{\bar{\alpha}^2 \tau^2}{x} \int_{x/x_c}^1 dz z \mathcal{K}(z) \left\{ \frac{1}{\sqrt{x_c - x/z}} - \frac{1}{\sqrt{x_c - x}} \right\}. \end{aligned} \quad (\text{A.3})$$

Let us denote by \mathcal{J} the integral in the second line above. After changing the integration variable according to $z = u/(u+1)$, this becomes

$$\mathcal{J} = \int_{x/x_c}^1 dz z \mathcal{K}(z) \left\{ \frac{1}{\sqrt{x_c - x/z}} - \frac{1}{\sqrt{x_c - x}} \right\} = \frac{1}{\sqrt{x_c - x}} \int_{u_0}^{\infty} du \left\{ \frac{1}{\sqrt{u - u_0}} - \frac{1}{\sqrt{u}} \right\}, \quad (\text{A.4})$$

where we denoted $u_0 \equiv x/(x_c - x)$. For any finite value of u_0 , the above integral over u is well defined and can be evaluated as

$$\begin{aligned} \mathcal{J} &= \frac{2}{\sqrt{x_c - x}} \lim_{u_M \rightarrow \infty} \left\{ \sqrt{u_M - u_0} - \sqrt{u_M} + \sqrt{u_0} \right\} \\ &= \frac{2}{\sqrt{x_c - x}} \lim_{u_M \rightarrow \infty} \left\{ \sqrt{u_0} - \frac{u_0}{2\sqrt{u_M}} \right\} = \frac{2\sqrt{x}}{x_c - x}, \end{aligned} \quad (\text{A.5})$$

where u_M is a sharp upper cutoff on u that has been introduced at intermediate steps in order to separate the two terms within the braces in the integral in Eq. (A.4). When inserting the final result from Eq. (A.5) into the second line of Eq. (A.3), one finds that it precisely cancels the other term there, so that the net result of this second iteration is exactly zero: $\mathcal{I}[D_{\text{rad}}^{(1)}] = 0$. Accordingly, the perturbative series becomes trivial (in the sense that all the higher order terms vanish) after the first iteration, and then the overall result is just the sum of the first two terms: $D_{\text{rad}} = D_{\text{rad}}^{(0)} + D_{\text{rad}}^{(1)}$. This is the result that has been announced towards the end of Sect. 4.2.

Now, the fact that the function $D_{\text{rad}}^{(1)}(x, \tau)$ is an exact fixed point of the branching term is indeed correct and should not be a surprise: in Sect. 4.3, we have seen that the very same function of x , namely $D_{\text{as}}(x) \propto 1/\sqrt{x(x_c - x)}$, emerges as the exact solution to the rate equation for the case of a source localized at $x = x_c$ (cf. Eq. (4.32)). Since the source vanishes at any $x < x_c$, this is tantamount to saying that $D_{\text{as}}(x)$ is an exact fixed point for the branching term: $\mathcal{I}[D_{\text{as}}] = 0$. This solution $D_{\text{as}}(x)$ becomes divergent when $x \rightarrow x_c$, but this is indeed a real property of that particular problem, because the respective source $\mathcal{S}(x) = A\delta(x - x_c)$ diverges at the end of the spectrum.

On the other hand, for the delocalized source $\mathcal{S}_0(x) = \bar{\alpha}/\sqrt{x}$, no such a divergence is expected (as also confirmed by the exact manipulations in Sect. 4.2), hence the iterative solution $D_{\text{rad}} = D_{\text{rad}}^{(0)} + D_{\text{rad}}^{(1)}$ cannot be fully right : it fails when $x \rightarrow x_c$. The mathematical reason for this failure can be traced to the subtlety of the limit $x \rightarrow x_c$ in relation with the manipulations in Eqs. (A.4)–(A.5): clearly, these manipulations become ambiguous when $x \rightarrow x_c$, or $u_0 \rightarrow \infty$, since this limit $u_0 \rightarrow \infty$ does not commute with the limit $u_M \rightarrow \infty$.

References

- [1] **ATLAS Collaboration**, G. Aad *et al.*, ‘‘Observation of a Centrality-Dependent Dijet Asymmetry in Lead-Lead Collisions at $\sqrt{s_{NN}} = 2.76$ TeV with the Atlas Detector at the LHC,’’ *Phys. Rev. Lett.* **105** (2010) 252303, [arXiv:1011.6182 \[hep-ex\]](#).

- [2] **CMS Collaboration**, S. Chatrchyan *et al.*, “Observation and Studies of Jet Quenching in PbPb Collisions at Nucleon-Nucleon Center-Of-Mass Energy = 2.76 TeV,” *Phys. Rev.* **C84** (2011) 024906, [arXiv:1102.1957 \[nucl-ex\]](#).
- [3] **CMS Collaboration**, S. Chatrchyan *et al.*, “Jet momentum dependence of jet quenching in PbPb collisions at $\sqrt{s_{NN}} = 2.76$ TeV,” *Phys.Lett.* **B712** (2012) 176–197, [arXiv:1202.5022 \[nucl-ex\]](#).
- [4] **ATLAS Collaboration**, G. Aad *et al.*, “Measurement of the jet radius and transverse momentum dependence of inclusive jet suppression in lead-lead collisions at $\sqrt{s_{NN}} = 2.76$ TeV with the ATLAS detector,” *Phys.Lett.* **B719** (2013) 220–241, [arXiv:1208.1967 \[hep-ex\]](#).
- [5] **CMS Collaboration**, S. Chatrchyan *et al.*, “Modification of jet shapes in PbPb collisions at $\sqrt{s_{NN}} = 2.76$ TeV,” *Phys.Lett.* **B730** (2014) 243–263, [arXiv:1310.0878 \[nucl-ex\]](#).
- [6] **CMS Collaboration**, S. Chatrchyan *et al.*, “Measurement of jet fragmentation in PbPb and pp collisions at $\sqrt{s_{NN}} = 2.76$ TeV,” [arXiv:1406.0932 \[nucl-ex\]](#).
- [7] **ATLAS Collaboration**, G. Aad *et al.*, “Measurement of inclusive jet charged-particle fragmentation functions in Pb+Pb collisions at $\sqrt{s_{NN}} = 2.76$ TeV with the ATLAS detector,” [arXiv:1406.2979 \[hep-ex\]](#).
- [8] **CMS Collaboration**, “Measurement of momentum flow relative to the dijet system in PbPb and pp collisions at $\sqrt{s_{NN}} = 2.76$ TeV,” *CMS PAS HIN-14-010* (2014) .
- [9] Y. Mehtar-Tani, C. A. Salgado, and K. Tywoniuk, “Antiangular Ordering of Gluon Radiation in QCD Media,” *Phys. Rev. Lett.* **106** (2011) 122002, [arXiv:1009.2965 \[hep-ph\]](#).
- [10] Y. Mehtar-Tani, C. A. Salgado, and K. Tywoniuk, “Jets in QCD Media: from Color Coherence to Decoherence,” *Phys. Lett.* **B707** (2012) 156–159, [arXiv:1102.4317 \[hep-ph\]](#).
- [11] J. Casalderrey-Solana, J. G. Milhano, and U. A. Wiedemann, “Jet Quenching via Jet Collimation,” *J.Phys.* **G38** (2011) 035006, [arXiv:1012.0745 \[hep-ph\]](#).
- [12] G.-Y. Qin and B. Muller, “Explanation of Di-jet asymmetry in Pb+Pb collisions at the Large Hadron Collider,” *Phys.Rev.Lett.* **106** (2011) 162302, [arXiv:1012.5280 \[hep-ph\]](#).
- [13] J. Casalderrey-Solana and E. Iancu, “Interference Effects in Medium-Induced Gluon Radiation,” *JHEP* **08** (2011) 015, [arXiv:1105.1760 \[hep-ph\]](#).
- [14] J.-P. Blaizot, F. Dominguez, E. Iancu, and Y. Mehtar-Tani, “Medium-induced gluon branching,” *JHEP* **1301** (2013) 143, [arXiv:1209.4585 \[hep-ph\]](#).
- [15] J. Casalderrey-Solana, Y. Mehtar-Tani, C. A. Salgado, and K. Tywoniuk, “New picture of jet quenching dictated by color coherence,” *Phys.Lett.* **B725** (2013) 357–360, [arXiv:1210.7765 \[hep-ph\]](#).
- [16] J.-P. Blaizot, E. Iancu, and Y. Mehtar-Tani, “Medium-induced QCD cascade: democratic branching and wave turbulence,” *Phys.Rev.Lett.* **111** (2013) 052001, [arXiv:1301.6102 \[hep-ph\]](#).
- [17] J.-P. Blaizot, F. Dominguez, E. Iancu, and Y. Mehtar-Tani, “Probabilistic picture for medium-induced jet evolution,” *JHEP* **1406** (2014) 075, [arXiv:1311.5823 \[hep-ph\]](#).
- [18] E. Iancu, “Di-jet asymmetry and wave turbulence,” [arXiv:1404.4566 \[hep-ph\]](#).
- [19] A. Kurkela and U. A. Wiedemann, “Picturing perturbative parton cascades in QCD matter,” [arXiv:1407.0293 \[hep-ph\]](#).
- [20] J.-P. Blaizot, Y. Mehtar-Tani, and M. A. C. Torres, “Angular structure of the in-medium QCD cascade,” [arXiv:1407.0326 \[hep-ph\]](#).
- [21] L. Apolinario, N. Armesto, J. G. Milhano, and C. A. Salgado, “Medium-induced gluon radiation and colour decoherence beyond the soft approximation,” [arXiv:1407.0599 \[hep-ph\]](#).

- [22] R. Baier, A. H. Mueller, D. Schiff, and D. Son, “‘Bottom up’ thermalization in heavy ion collisions,” *Phys.Lett.* **B502** (2001) 51–58, [arXiv:hep-ph/0009237 \[hep-ph\]](#).
- [23] S. Jeon and G. D. Moore, “Energy loss of leading partons in a thermal QCD medium,” *Phys.Rev.* **C71** (2005) 034901, [arXiv:hep-ph/0309332 \[hep-ph\]](#).
- [24] R. Baier, Y. L. Dokshitzer, A. H. Mueller, S. Peigne, and D. Schiff, “Radiative Energy Loss of High Energy Quarks and Gluons in a Finite-Volume Quark-Gluon Plasma,” *Nucl. Phys.* **B483** (1997) 291–320, [arXiv:hep-ph/9607355](#).
- [25] R. Baier, Y. L. Dokshitzer, A. H. Mueller, S. Peigne, and D. Schiff, “Radiative Energy Loss and P(T)-Broadening of High Energy Partons in Nuclei,” *Nucl. Phys.* **B484** (1997) 265–282, [arXiv:hep-ph/9608322](#).
- [26] B. G. Zakharov, “Fully Quantum Treatment of the Landau-Pomeranchuk-Migdal Effect in QED and QCD,” *JETP Lett.* **63** (1996) 952–957, [arXiv:hep-ph/9607440](#).
- [27] B. G. Zakharov, “Radiative Energy Loss of High Energy Quarks in Finite-Size Nuclear Matter and Quark-Gluon Plasma,” *JETP Lett.* **65** (1997) 615–620, [arXiv:hep-ph/9704255](#).
- [28] R. Baier, Y. L. Dokshitzer, A. H. Mueller, and D. Schiff, “Medium-Induced Radiative Energy Loss: Equivalence Between the Bdmgs and Zakharov Formalisms,” *Nucl. Phys.* **B531** (1998) 403–425, [arXiv:hep-ph/9804212](#).
- [29] V. Zakharov, V. Lvov, and G. Falkovich, “Kolmogorov spectra of turbulence, Volume 1,” *Springer-Verlag* (1992) 264 p.
- [30] S. Nazarenko, “Wave Turbulence,” *Springer-Verlag, Berlin* (2011) 279 p.
- [31] A. Kurkela and G. D. Moore, “Thermalization in Weakly Coupled Nonabelian Plasmas,” *JHEP* **1112** (2011) 044, [arXiv:1107.5050 \[hep-ph\]](#).
- [32] C. A. Salgado and U. A. Wiedemann, “Medium modification of jet shapes and jet multiplicities,” *Phys.Rev.Lett.* **93** (2004) 042301, [arXiv:hep-ph/0310079 \[hep-ph\]](#).
- [33] K. M. Burke, A. Buzzatti, N. Chang, C. Gale, M. Gyulassy, *et al.*, “Extracting jet transport coefficient from jet quenching at RHIC and LHC,” *Phys.Rev.* **C90** (2014) 014909, [arXiv:1312.5003 \[nucl-th\]](#).
- [34] B. Schenke, C. Gale, and S. Jeon, “Martini: an Event Generator for Relativistic Heavy-Ion Collisions,” *Phys. Rev.* **C80** (2009) 054913, [arXiv:0909.2037 \[hep-ph\]](#).
- [35] T. Liou, A. Mueller, and B. Wu, “Radiative p_{\perp} -broadening of high-energy quarks and gluons in QCD matter,” *Nucl.Phys.* **A916** (2013) 102–125, [arXiv:1304.7677 \[hep-ph\]](#).
- [36] E. Iancu, “The non-linear evolution of jet quenching,” [arXiv:1403.1996 \[hep-ph\]](#).
- [37] J.-P. Blaizot and Y. Mehtar-Tani, “Renormalization of the jet-quenching parameter,” [arXiv:1403.2323 \[hep-ph\]](#).
- [38] E. Iancu and D. Triantafyllopoulos, “Running coupling effects in the evolution of jet quenching,” [arXiv:1405.3525 \[hep-ph\]](#).
- [39] B. Wu, “Radiative energy loss and radiative p_T -broadening of high-energy partons in QCD matter,” [arXiv:1408.5459 \[hep-ph\]](#).
- [40] R. Baier, Y. L. Dokshitzer, A. H. Mueller, and D. Schiff, “Quenching of hadron spectra in media,” *JHEP* **0109** (2001) 033, [arXiv:hep-ph/0106347 \[hep-ph\]](#).
- [41] D. Binosi and L. Theussl, “JaxoDraw: A Graphical user interface for drawing Feynman diagrams,” *Comput.Phys.Commun.* **161** (2004) 76–86, [arXiv:hep-ph/0309015 \[hep-ph\]](#).